DOE/MC/30012 -- 5305

# Advanced Sulfur Control Concepts in Hot-Gas Desulfurization Technology

## Quarterly Report
## January 1 - March 31, 1996



Work Performed Under Contract No.: DE-AC21-94MC30012

For
U.S. Department of Energy
Office of Fossil Energy
Morgantown Energy Technology Center
P.O. Box 880
Morgantown, West Virginia 26507-0880

By
Louisiana State University
Department of Chemical Engineering
Baton Rouge, Louisiana 70803-7303



# Disclaimer

## EXECUTIVE SUMMARY

The last experimental tests involving FeS regeneration in both the atmospheric pressure and high pressure electrobalance reactors were completed during the quarter. The effects of temperature, reactant composition, and flow rate were studied in the atmospheric pressure electrobalance in atmospheres of $O_2/N_2$, $H_2O/N_2$, and $O_2/H_2O/N_2$. The same parameters plus pressure were studied in the high pressure electrobalance. Essentially all runs were carried out at volumetric flow rates sufficiently large to eliminate external mass transfer resistance. The initial regeneration rate was found to be a weak function of temperature and to be first-order in both $O_2$ and $H_2O$. In tests involving both $O_2$ and $H_2O$, the initial reaction rate was equal to the sum of the individual rates involving $O_2$ only and $H_2O$ only. The effect of pressure on the initial reaction rates in high pressure tests was somewhat unexpected in that the initial rate increased with pressure between 1 and 5 atm, and subsequently decreased between 5 and 15 atm.

Statistical analysis and correlation of the electrobalance data have been completed and results are presented in this report. Equations for the initial rate of regeneration of FeS in $O_2$ and $H_2O$ as a function of temperature and reactive gas concentration have been developed.

Slow progress has been made with the fixed-bed reactor. A number of reactor scoping tests involving FeS regeneration in $O_2$ and $H_2O$, and $CeO_2$ sulfidation in $H_2S$ were completed during the quarter. Chromatographic product gas analysis is now working reliably. Final repairs on the PMT temperature controller for the Antek total sulfur analyzer were completed and the unit seems to be functioning as expected. The Antek and GC responses in FeS regeneration runs in which all sulfur should be liberated as $SO_2$ tracked reasonably well.

Our primary concern at the end of the quarter is the fragility of the quartz pyrotubes and our ability to maintain constant flow rate to the Antek analyzer. The reaction systems are inherently dirty. Particles produced by corrosion of metal components and deposition of solid sulfur have resulted in plugging problems in both the pyrotube and reactor product lines leading to the chromatograph. Partial plugging of the pyrotube causes a reduction in flow rate to the total sulfur analyzer and alters the response of the instrument. For this reason, we have abandoned our original plan to use a generalized flow rate versus pressure calibration curve. Instead, the flow rate associated with each individual test will be measured. We are also investigating the feasibility of having a $SiO_2$-coated stainless steel flow restrictor and pyrotube fabricated in order to avoid the breakage problems experienced with quartz.

## GAS ANALYSIS

We continued to work with Antek during the quarter to solve problems with the total sulfur analyzer. The temperature controller on the photomultiplier tube was replaced a second time and the unit is now capable of holding the desired 10°C operating temperature. In addition, Antek supplied a new pyrotube in which the capillary restrictor was packed with ceramic powder to increase the resistance and decrease the flow rate. Initial tests were

promising but the quartz entrance tube was broken before testing was complete. We are awaiting its repair at the end of the quarter. The fragility of these quartz pyrotubes is of continuing concern, and has prompted us to investigate the fabrication of a $SiO_2$-coated stainless steel flow restrictor and pyrotube. One-sixteenth inch outside diameter by 0.004 inch inside diameter stainless steel capillary tubing would serve as the flow restrictor. The stainless steel portion can be fabricated in the LSU shops and surfaces of the unit exposed to corrosive gas would be coated with $SiO_2$ by Restec Corporation in Bellefonte, Pennsylvania. While this approach should eliminate the quartz breakage problems, questions about the stability of the $SiO_2$-steel bond at the severe conditions of our test remain.

Reaction tests using the total sulfur analyzer, which are described in the following section of this report, used the original unpacked quartz flow restrictor. In order to avoid saturating the UV fluorescence detector, $N_2$ dilution, as shown in Figure 1 and discussed in the previous quarterly report, was utilized. The system was recalibrated at an inlet pressure, P1=50 psig which produced a flow rate of Q1=25 sccm. Flow rates of $O_2$, Q2=437 sccm, and diluent $N_2$, Q3=371 sccm, were used. Twenty-three calibration points having $H_2S$ mol fractions between 0.005 and 0.0848 were measured. Results are shown in Figure 2.

The calibration points were regressed using a quadratic equation to give

$$y = 8 + 169.4x - 8.786x^2 \qquad (1)$$

where y is the Antek reading and x is the mol percent $H_2S$. Reversing the equation to solve for percent $H_2S$ corresponding to a given Antek reading gives

$$x = 9.64 - 5.09\times10^{3}\,(3.62\times10^{6} - 4393y)^{0.5} \qquad (2)$$

The average percent difference between analyzer $H_2S$ percent and feed $H_2S$ percent (as determined by flow controller settings) is +1.7% for the 23 calibration points. The range in percent difference is from -6.2% to +20.9%, and the difference is less than $\pm$7% for 21 of the 23 points.

It also proved necessary to recalibrate the gas chromatograph during the quarter. Originally, the current to the TCD was too large, and the unit automatically tripped off at times. Calibration curves at a lower detector current are shown in Figure 3. The calibration was linear and the equations relating peak area and percent $SO_2$ and $H_2S$ are

$$\%\ SO_2 = 4.142\times10^{-6}\ \text{Area} \qquad (3)$$

$$\%\ H_2S = 5.390\times10^{-6}\ \text{Area} \qquad (4)$$

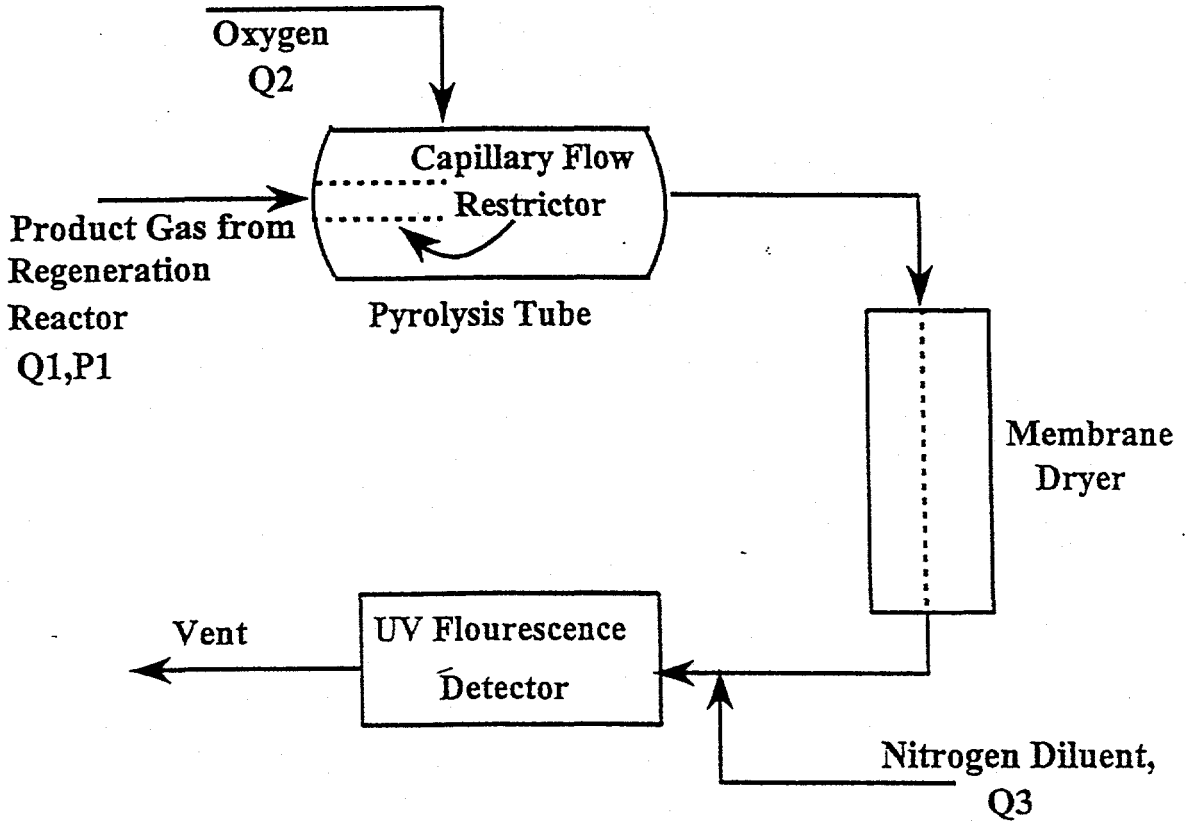


Figure 1. Simplified Flow Diagram of the Antek Total Sulfur Analyzer Showing $N_2$ Dilution of the Pyrotube Exit Gas

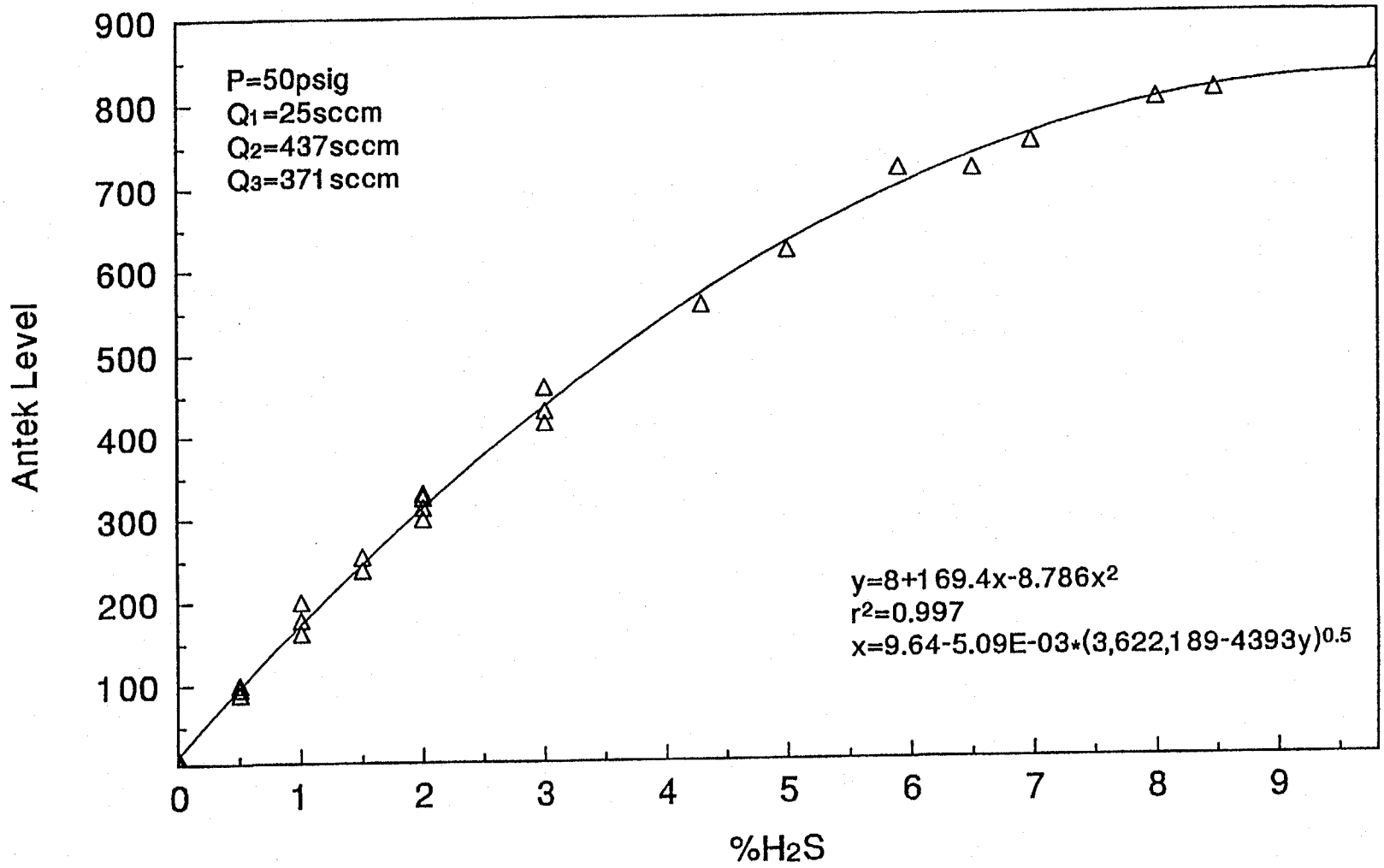


Figure 2. Calibration Curve for the Antek Total Sulfur Analyzer

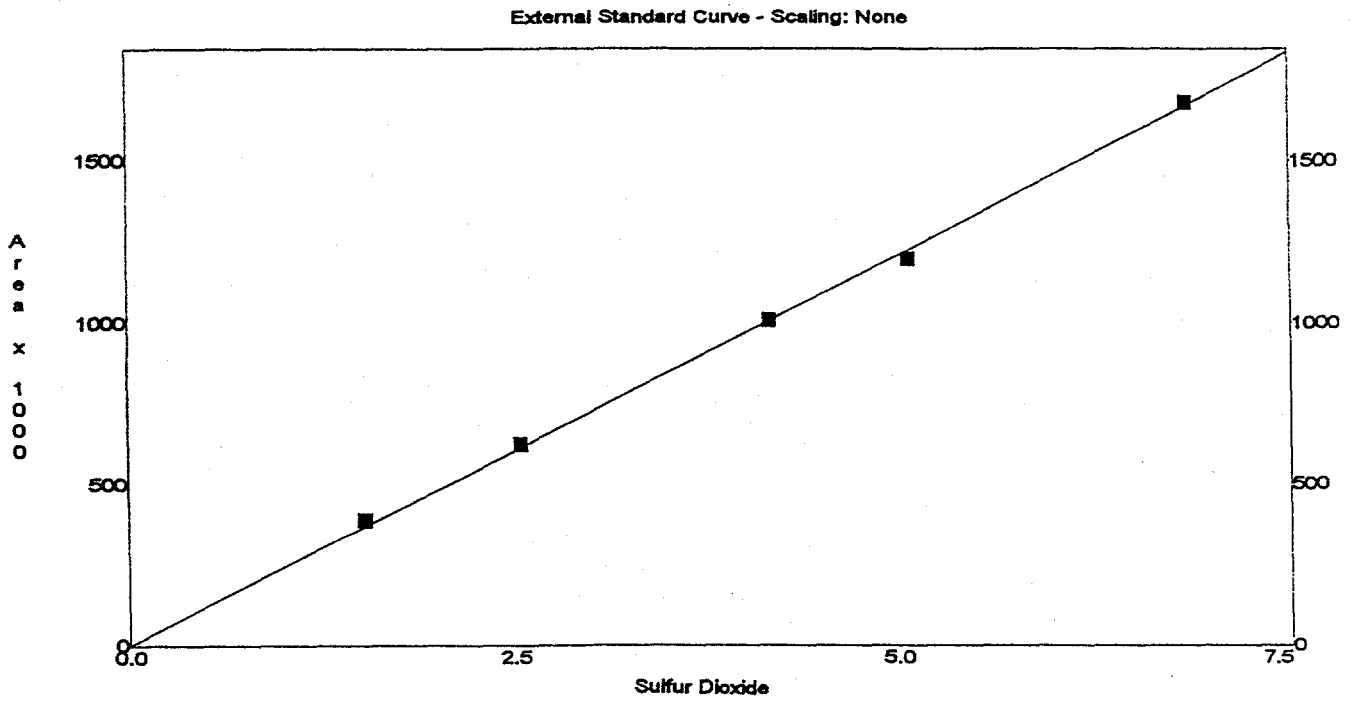


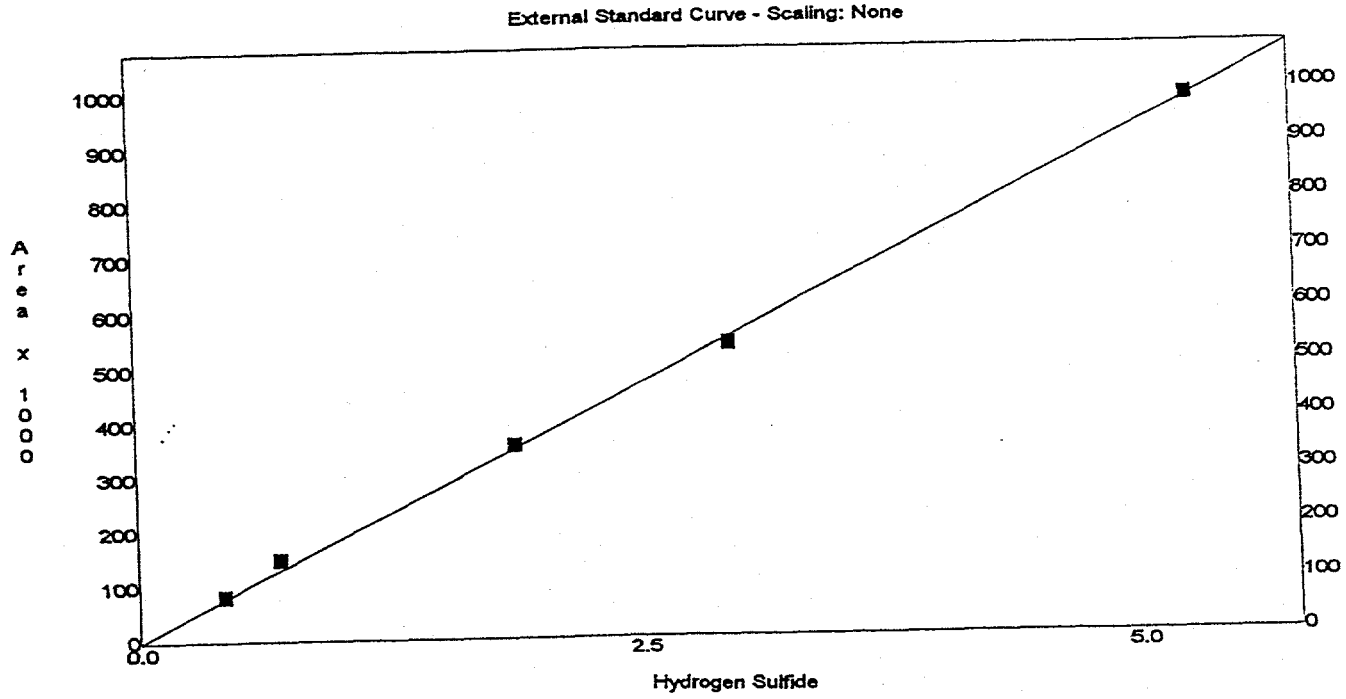


Figure 3. GC Calibration Curves for $SO_2$ and $H_2S$

These constants are approximately 15% smaller than previous calibration constants using higher detector current.

## FIXED-BED REACTOR SCOPING TESTS

Reactor scoping tests were initiated during January. These tests have been carried out under increasingly severe conditions in order to evaluate components of the reactor and gas analysis systems. Key potential problem areas anticipated in the reactor system included the stability of the o-rings at the high reaction temperatures, our ability to vaporize steam and then prevent its condensation on cool surfaces near the top of the reactor, and our ability to handle elemental sulfur produced during sorbent regeneration. The elemental sulfur present in that portion of the reactor product which is fed to the Antek unit must remain in the vapor phase until it reaches the pyrotube where it reacts with $O_2$ to form $SO_2$. Elemental sulfur in the remainder of the reactor product must be kept in the vapor phase until it reaches the condenser. There the elemental sulfur must be removed to avoid plugging cooler downstream lines which lead to the backpressure regulator and gas chromatograph. Tests completed by the end of the quarter have shown that Aflas o-rings are stable at reaction conditions of at least 750°C and 4.4 atm. $H_2O$ condensation problems were experienced when in the feed gas contained steam. In such cases it is necessary to insure that the upper portion of the reactor is sufficiently hot to prevent condensation but not too hot to destroy the o-rings. While this requirement will require careful control, we believe that it can be satisfied.

Regeneration scoping tests completed during the quarter were such that the majority of the sulfur should be liberated as $SO_2$ or $H_2S$, with only small amounts of elemental sulfur. Therefore, our ability to handle elemental sulfur in the regenerator product has not yet been evaluated.

### FeS Regeneration Tests

Eleven FeS regeneration scoping tests were completed during the quarter; reaction conditions are summarized in Table 1.

Tests FeS-01 and FeS-02 were carried out at 16.3 atm with a feed gas containing 1% $O_2$ in $N_2$. Temperature was varied during the reaction from a minimum of 300°C at the beginning of FeS-01 to 500°C at the end of FeS-02. No $SO_2$ was detected at 300°C or 350°C, and small quantities ($\sim$0.001 mol fraction) were detected at 400°C. The temperature in FeS-02 varied from 450°C initially to 500°C at the end. The $SO_2$ content of the product gas (as determined by GC analysis) reach 0.0052 mol fraction near the end of the test. The maximum mol fraction of $SO_2$, based upon complete conversion of $O_2$ to form $Fe_2O_3$ and $SO_2$, is 0.0057. It is possible that some of the difference may be due to $Fe_2(SO_4)_3$ formation at these reaction conditions. The

Table 1. Summary of Fixed-Bed Reactor Test Conditions: FeS Regeneration

| Run | FeS-01 | FeS-02 | FeS-03 | FeS-04 | FeS-05 | FeS-06 | FeS-07 | FeS-08 | FeS-09 | FeS-10 | FeS-11 |
|---|---|---|---|---|---|---|---|---|---|---|---|
| Date | 1-29-96 | 2-5-96 | 2-8-96 | 2-12-96 | 2-14-96 | 2-16-96 | 2-21-96 | 2-26-96 | 2-28-96 | 3-1-96 | 3-8-96 |
| Reactor Packing | | | | | | | | | | | |
| FeS, g | 24.2 | 24.4 | 8.84 | 5.97 | 5.97 | 6.00 | 3.26 | 3.27 | 3.20 | 3.20 | 3.27 |
| $Al_2O_3$,g | -- | -- | -- | -- | -- | -- | 3.29 | 3.26 | 3.22 | 3.22 | 3.29 |
| Reaction Conditions | | | | | | | | | | | |
| Temp., °C | 300→420 | 450→500 | 500 | 550 | 600 | 600 | 600 | 600 | 650 | 700 | 600 |
| Press., atm | 16.3 | 16.3 | 16.5 | 16.7 | 16.7 | 4.4 | 4.4 | 4.4 | 4.5 | 4.7 | 4.4 |
| Gas Comp. | | | | | | | | | | | |
| $\%O_2$ | 1.0 | 1.0 | 1.0 | 1.5 | 1.5 | 1.5 | 1.5 | -- | -- | -- | 1.5 |
| % $H_2O$ | -- | -- | -- | -- | -- | -- | -- | 5→10 | 10.0 | 10.0 | -- |
| % $N_2$ | 99.0 | 99.0 | 99.0 | 98.5 | 98.5 | 98.5 | 98.5 | 95→90 | 90.0 | 90.0 | 98.5 |
| Gas Flow, sccm | 600 | 600 | 1050 | 600 | 600 | 600 | 600 | 600→1800 | 600 | 600 | 600 |
| Space Velocity, $hr^{-1}$ at STP | 2050 | 2050 | 12500 | 13650 | 13650 | 13650 | 6500 | 6500 | 7200 | 6500 | 6500 |

o-rings were somewhat distorted after these runs but they regained their circular cross-section with time and were used in a subsequent run without any trouble.

Run FeS-03 was the first in which all reaction conditions were held constant throughout the run. Pressure was 16.5 atm and temperature was 500°C. The FeS charge was reduced to 8.84 grams and the volumetric feed rate increased to 1050 sccm. The feed composition was 1% $O_2$ in $N_2$. The reactor response, in terms of mol fraction of $SO_2$ in the product gas versus dimensionless time, is shown in Figure 4. Dimensionless time is defined by the following equation

$$t^* = \frac{0.57\ n_G\ y_{O_2}\ t}{n_{FeS}} \qquad (5)$$

where 0.57 is the ratio of the stoichiometric coefficient of FeS to that of $O_2$ from the equation

$$2FeS + \frac{7}{2}O_2 \rightarrow Fe_2O_3 + 2SO_2, \qquad (6)$$

$n_G$ is the total gas feed rate, mol/min, $y_{O_2}$ is the mol fraction $O_2$ in the feed gas, $n_{FeS}$ is the mols of FeS initially charged to the reactor, and t is the reaction time. $t^*$ is defined so that $t^*=1$ would correspond to complete conversion of FeS to $Fe_2O_3$ if the reaction proceeded as written at an infinite rate. Viewed alternately, $t^*=1$ corresponds to the time at which the cumulative amount of $O_2$ fed is just sufficient to convert all FeS to $Fe_2O_3$. For the conditions of test FeS-03, $t^*=1$ corresponds to an elapsed run time of 7.5 hours.

From Figure 4, we see that $SO_2$ first appeared in the product gas at $t^* \sim 0.05$ ($t \sim 0.375$ hr). The $SO_2$ content increased rapidly, reached a maximum of 0.0046 mol fraction at $t^*=0.095$ ($t=0.72$ hr), and declined slowly thereafter. The run was terminated after $t^* \sim 1.02$ hrs ($t \sim 7.65$ hr) with the mol fraction of $SO_2$ in the product gas equal to 0.0015. The cumulative $SO_2$ produced, measured as a fraction of the stoichiometric $SO_2$, was equal to 0.28.

Several changes were made in reaction conditions for tests FeS-04 and FeS-05. The reaction temperature was increased in 50°C increments to 550°C in FeS-04 and to 600°C in FeS-05. The initial charge of FeS was further reduced to 5.97g in each test, the $H_2S$ content of the feed was increased to 0.015 mol fraction, and the total volumetric feed rate was reduced to 600 sccm. These changes reduced the elapsed reaction time corresponding to $t^*=1$ to 4.9 hours. The reactor response was qualitatively similar in both tests with results from test FeS-05 illustrated in Figure 5. After a short delay, the $SO_2$ content of the product gas increased rapidly, reached a maximum of 0.0088 mol fraction, and decreased slowly thereafter. The maximum experimental $SO_2$ mol fraction was 103% of the theoretical maximum of 0.0086. Run FeS-05 was terminated at $t^*=1.3$, corresponding to an elapsed time of 6.4 hours. The cumulative amount of $SO_2$ produced was 68% of the stoichiometric quantity. At the conclusion of test FeS-05, the o-rings were stuck in the o-ring grooves and had to be peeled away. Once again, the

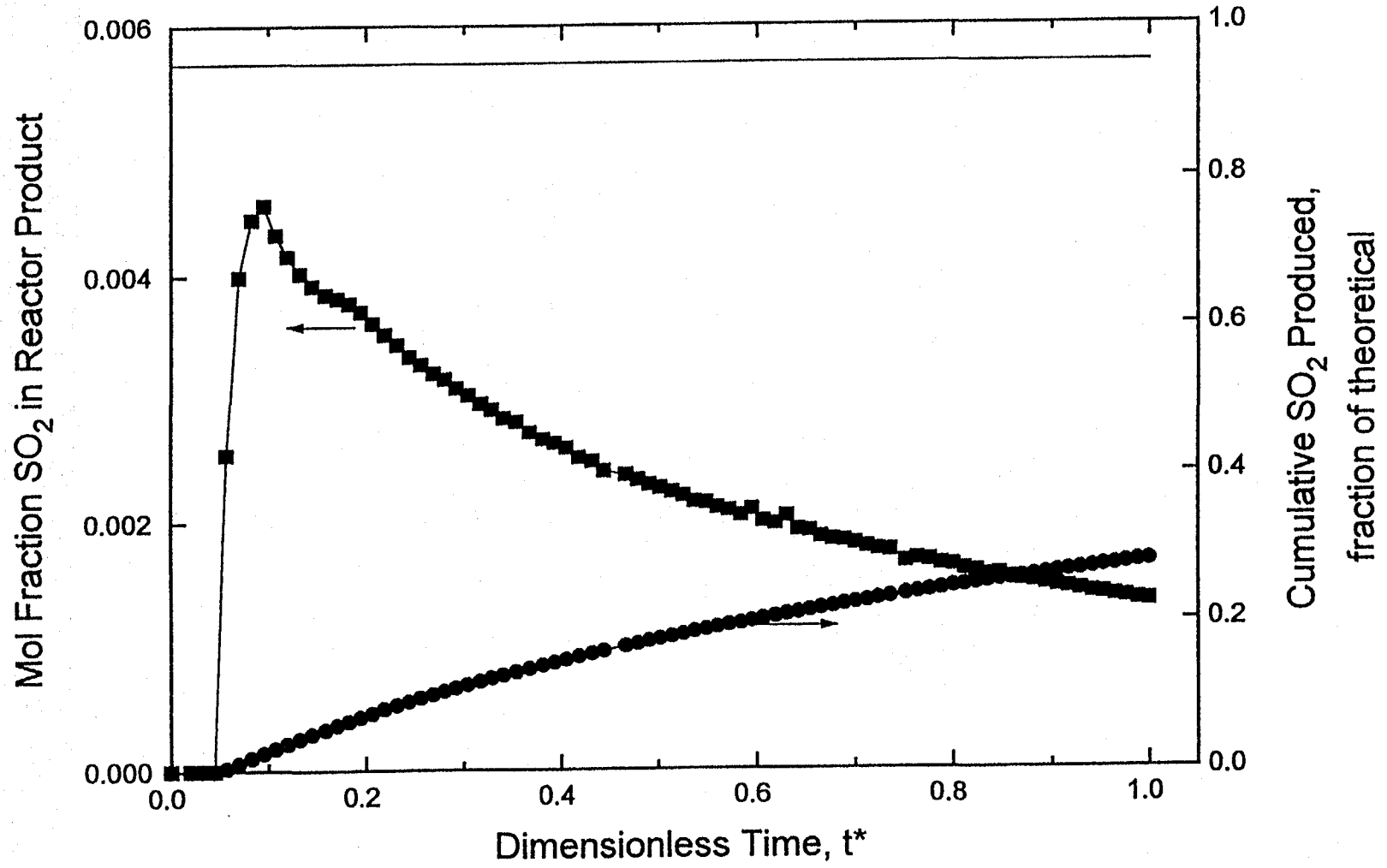


Figure 4. Fixed-Bed Reactor Resposne: Test FeS-03

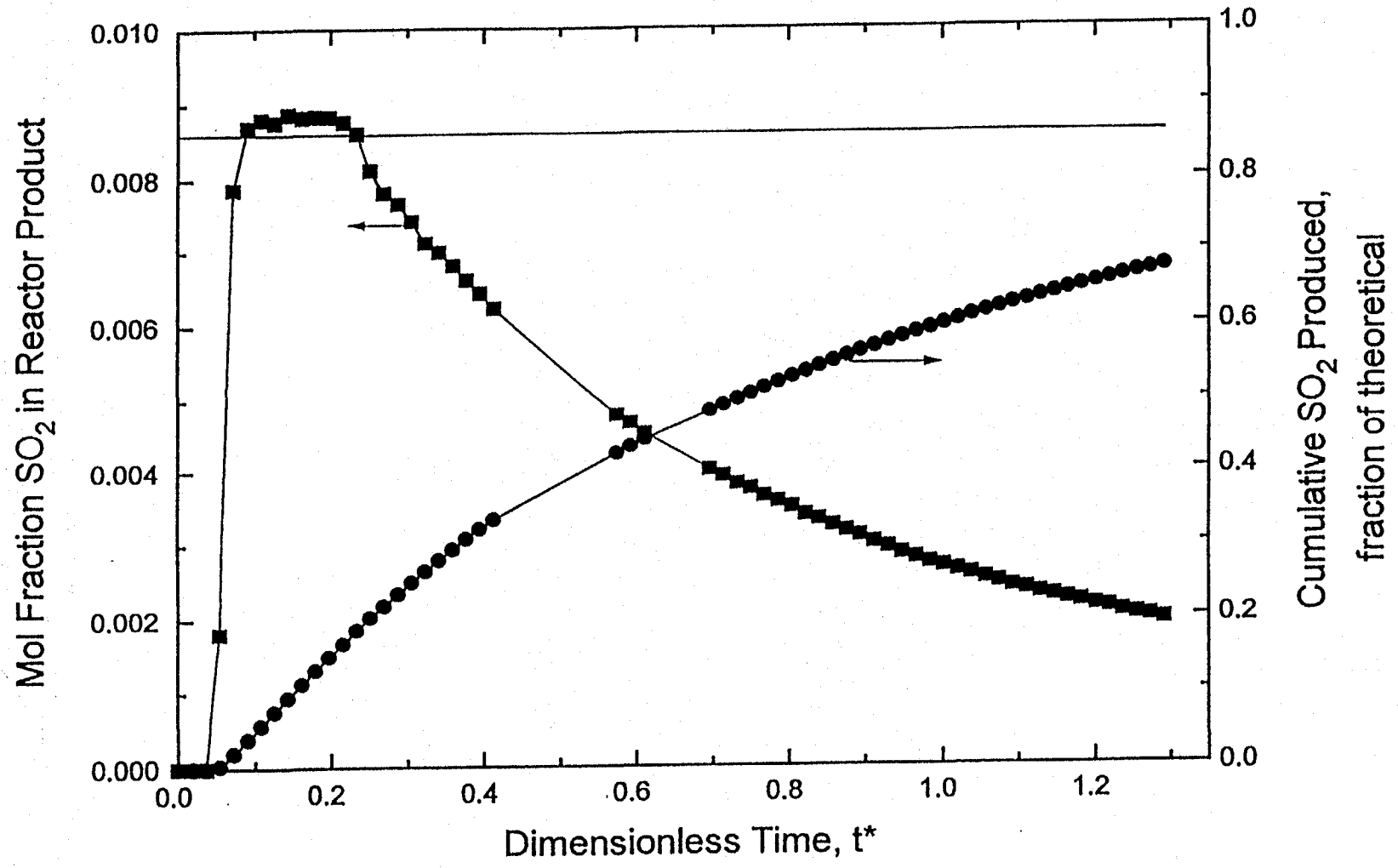


Figure 5. Fixed-Bed Reactor Response: Test FeS-05

o-rings regained their circular cross-section with time, and they were successfully re-used in a later test.

Reactor pressure was reduced to 4.4 atm in test FeS-06, while other reaction conditions were the same as in test FeS-05. Reactor response was similar. After a brief delay the $SO_2$ content of the product gas increased rapidly, reached a maximum of 0.0087 mol fraction, and decreased slowly thereafter. When the test was terminated at $t^*=1.24$, the cumulative $SO_2$ produced was 71% of theoretical.

The sorbents removed from the reactor at the conclusion of tests FeS-02 through FeS-06 were badly sintered. Free-flowing FeS powder was added initially, but the product emerged as a solid cylindrical rod. We attribute the lack of complete regeneration at reaction times significantly greater than $t^*=1.0$ to sintering, which limited the access of $O_2$ to unreacted FeS.

In order to minimize sintering, the FeS was diluted with an approximately equal quantity of inert $Al_2O_3$ beginning in test FeS-07. Other reaction conditions in tests FeS-07 and FeS-06 were the same. The response curve from test FeS-07 is shown in Figure 6. The $SO_2$ concentration increased rapidly soon after the reaction began and exceeded 0.008 mol fraction over the period $0.13 \leq t^* \leq 0.91$. The theoretical maximum $SO_2$ mol fraction of 0.0086 was exceeded for the period $0.18 \leq t^* \leq 0.90$. During most of this time the experimental mol fraction was approximately constant at 102% of theoretical, but increased to about 108% of theoretical at $t^* \sim 0.8$. $SO_2$ concentration quickly decreased beginning at $t^* \sim 0.9$ and approached zero at $t^* \sim 1.2$. The total quantity of $SO_2$ produced during the test was about 96% of the theoretical quantity.

The fact that the $SO_2$ content exceeded theoretical for a large portion of the run is consistent with the formation-decomposition of $Fe_2(SO_4)_3$. $Fe_2(SO_4)_3$ may be formed initially near the entrance of the bed when temperatures and partial pressures of $O_2$ and $SO_2$ are favorable. As time increases, the $SO_2$ concentration near the reactor entrance is reduced, leading to $Fe_2(SO_4)_3$ decomposition. As decomposition occurs near the entrance, conditions become favorable for its formation further into the bed, and $Fe_2(SO_4)_3$ tends to move through the bed with time. As the $Fe_2(SO_4)_3$ zone approaches the bed exit, there is decreased opportunity for it to be reformed and the $SO_2$ concentration in the product gas increases. While this is a logical explanation of the observed behavior, it has not been confirmed by direct analysis of the presence or absence of $Fe_2(SO_4)_3$.

The use of the FeS-$Al_2O_3$ mixture eliminated, or at least greatly reduced, sintering. The solid was easily removed from the reactor and only a few small, lightly bound clumps were present. The addition of $Al_2O_3$ is believed responsible for the much improved reactor response in FeS-07, which is characterized by the extended time during which large $SO_2$ concentrations were measured, and the fact that essentially all of the sulfur in the initial FeS charge was converted to $SO_2$.

In runs FeS-08 through FeS-10, the feed gas composition was switched from $O_2/N_2$ to $H_2O/N_2$. Under these conditions, the products of regeneration should be solid $Fe_3O_4$ and gaseous

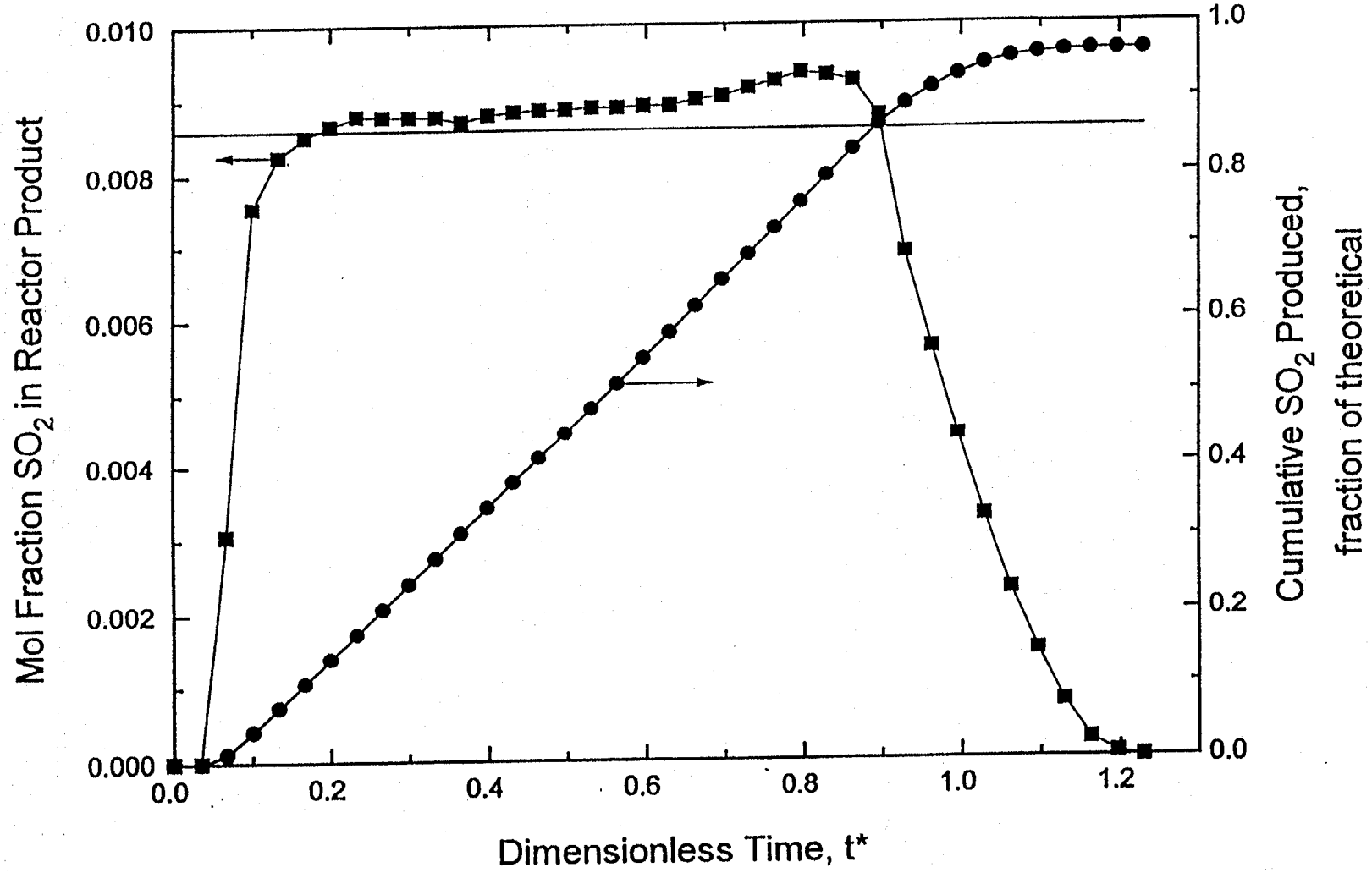


Figure 6. Fixed-Bed Reactor Response: Test FeS-07

$H_2S$ and $H_2$ (3 mol $H_2S$ per mol $H_2$). The relationship between reaction time and dimensionless time is given by

$$t^* = \frac{0.75\ n_G\ y_{H_2O} t}{n_{FeS}} \qquad (7)$$

The ratio of stoichiometric coefficients is changed, but other terms are the same as in eqn. (5). In run FeS-08 both the total gas feed rate and the $H_2O$ mol fraction were varied. $H_2S$ was formed, but the maximum mol fraction in the product gas was about 0.001, considerably below the 0.0375 theoretical value associated with complete conversion of 0.05 mol fraction $H_2O$ in the feed gas. The low $H_2S$ concentration was not unexpected on the basis of electrobalance results showing that the rate of reaction of FeS with $H_2O$ is small compared to the rate of FeS with $O_2$.

In run FeS-09, which used constant reaction conditions, the mol fraction of $H_2O$ in the feed was 0.10 and the temperature was increased to 650°C. Reaction time corresponding to $t^*=1$ was only 0.3 hr because of the large $H_2O$ feed rate. The reactor response, shown in Figure 7, was characterized by highly variable $H_2S$ concentration during the period $t^* \leq 8$, followed by a period during which the $H_2S$ mol fraction was relatively constant at about 0.0015. The cumulative quantity of $H_2S$ produced during the reaction was only 29% of theoretical, even though the total reaction time corresponded to $t^*=15$. The large variation in $H_2S$ concentration during the early stages is attributed to uneven steam concentrations in the gas reaching the sorbent bed. We believe that steam condensed on cool surfaces in the upper portion of the reactor during this period. Periodically, drops of water fell into the heated zone where they vaporized and produced widely varying steam concentrations. The temperature of gas near the top of the pressure vessel is also shown in Figure 7. This temperature increased gradually from about 80°C at the beginning of the reaction to about 110°C near the end. This temperature reached about 100°C at $t^*=8$, and from that time, the $H_2S$ concentrations were, with one exception, relatively constant. Better insulation will result in higher temperature near the top of the reactor. This solution must be approached cautiously, however, as the o-rings are in this same general area.

In test FeS-10, the reaction temperature was increased by another 50°C to 700°C and all insulation was removed from the top of the pressure vessel. The gas temperature near the top of the reactor never exceeded 93°C and the $H_2S$ concentration in the product was variable throughout the run.

Test FeS-11 represented the first attempt to determine the reproducibility of the reactor response. Oxygen was again used as the reactive gas and reaction conditions were identical to those used in test FeS-07. In addition, both the Antek total sulfur analyzer and the gas chromatograph were used to analyze the sulfur content of the product gas. Since essentially all of the gas phase sulfur should appear as $SO_2$, the two analyzers should give the same results.

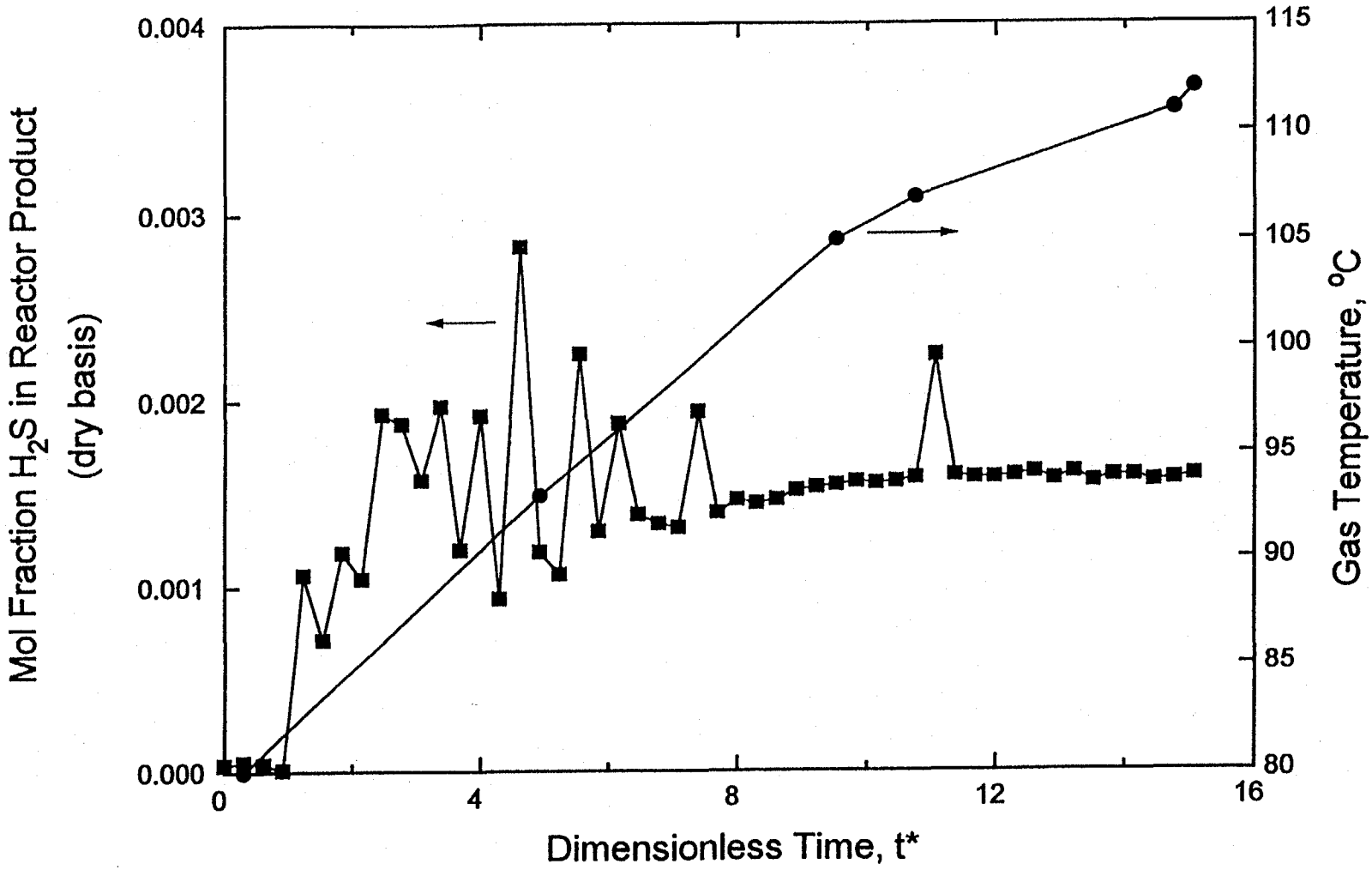


Figure 7. Reactor Response: Test FeS-09

The results from gas chromatographic analysis of tests FeS-07 and FeS-11 are compared in Figure 8. In both runs the $SO_2$ concentration increased rapidly beginning about $t^*=0.05$, was relatively constant between $0.2 \leq t^* \leq 0.8$, and decreased over the period $0.8 \leq t^* \leq 1.3$. The $SO_2$ concentration during the "steady-state" period was approximately 3% larger in run FeS-07, and the concentration decay rate was somewhat slower in run FeS-11. The sulfur material balance closure was comparable in both tests, with the cumulative $SO_2$ produced in FeS-07 equal to 96% of theoretical compared to 92% of theoretical in FeS-11.

The agreement between the GC and total sulfur analyzer in test FeS-11 was not as good as hoped. These results are compared in Figure 9. While $SO_2$ appeared and then disappeared in the product gas at about the same time, the "steady-state" $SO_2$ mol fraction was about 0.007 from the total sulfur analyzer compared to about 0.0085 from the chromatograph. The 0.0085 value is more believable because it is near the theoretical mol fraction and because it is close agreement with the results from FeS-07. The low readings from the total sulfur analyzer are probably caused by reduced flow rate of product gas through the capillary flow restrictor. The flow rate used to calculate the concentrations shown in Figure 9 was based upon a flow rate-pressure calibration curve developed several months ago. Since the reaction system is inherently dirty, and since periodic problems with plugging of lines and valves have occurred, we believe the actual flow rate to be less than indicated by the calibration curve. In order to minimize this problem in future, we plan to measure the flow rate through the capillary restrictor for each run.

## $CeO_2$ Sulfidation Tests

Fixed-bed reactor scoping tests then shifted to $CeO_2$ sulfidation. Four tests were completed during the quarter and reaction conditions are summarized in Table 2.

Test $CeO_2$-01 represented the first time that $CeO_2$ had been used and the first time that $H_2S$ was fed at potentially reactive conditions. Hydrogen was included in the feed both to minimize decomposition of $H_2S$ and since it is required for the reaction.

$$2CeO_2 + H_2S + H_2 \rightarrow Ce_2O_2S + 2H_2O \qquad (8)$$

Pressure, feed gas composition, and flow rate were held constant while the temperature was increased from 300°C at the beginning of the test to 700°C at the end. Only the gas chromatograph was used for product gas analysis as we did not wish to feed large $H_2$ concentrations to the Antek unit. It was clear that no significant reaction between $CeO_2$ and $H_2S$ occurred at low temperatures, but the results were uncertain at high temperatures. The unexpected result was that the solid product was pyrophoric when it was removed from the reactor and brought into contact with air. This is now thought to be associated with the reduction of $CeO_2$ by $H_2$ to non-stoichiometric forms represented by the formula $CeO_{2-x}$.

Run $Ce_2O_2$-02 was carried out isothermally at 650°C; other reaction conditions were the same as in test $CeO_2$-01. There was some indication of reaction at these conditions, but the extent was much lower than desired.

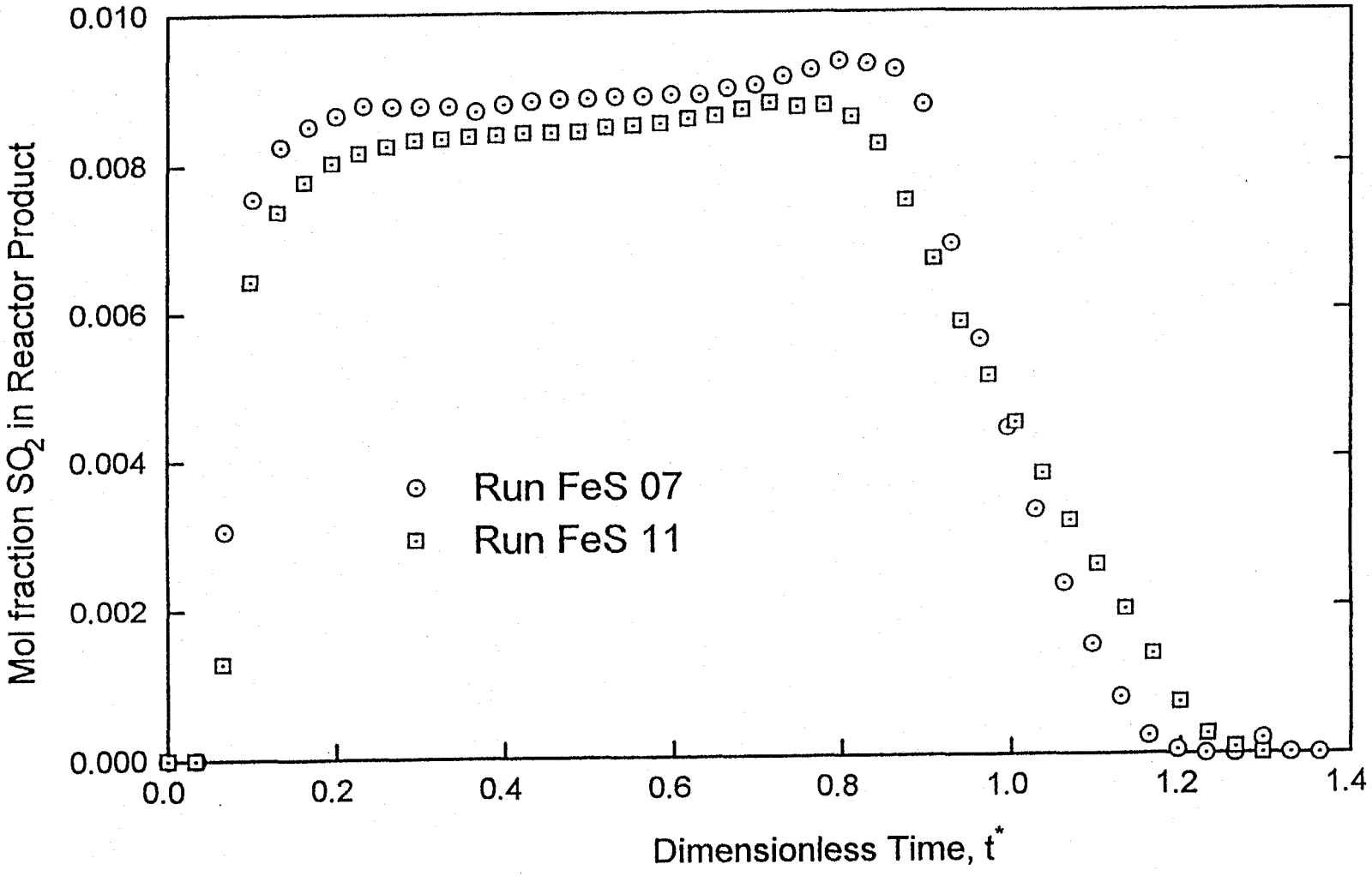


Figure 8. Comparison of Fixed-Bed Reactor Response for Duplicate Tests FeS-07 and FeS-11: Gas Chromatographic Analysis

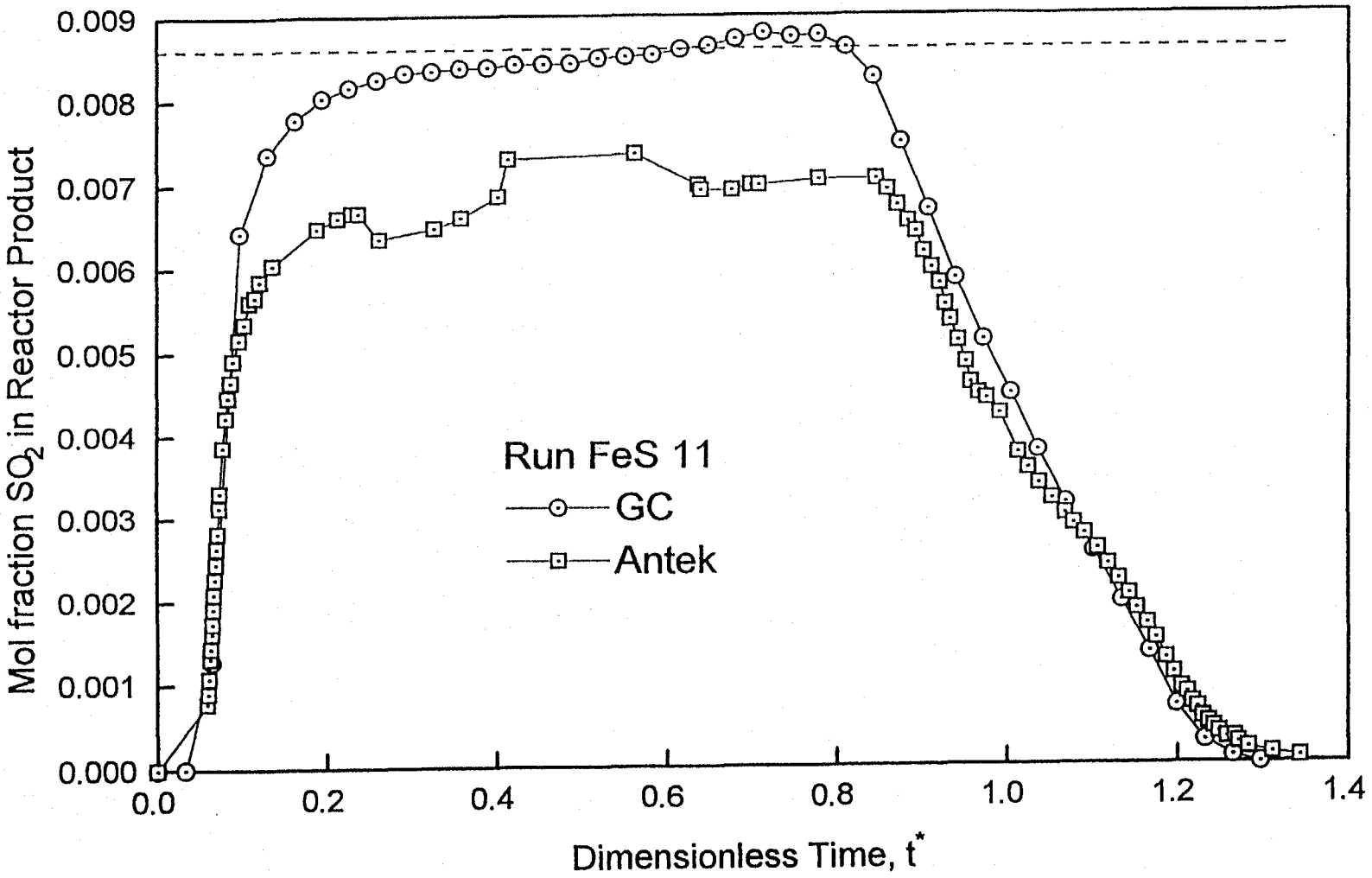


Figure 9. Comparison of the Reactor Response for Test FeS-11 as Determined by GC and Antek Analysis

Table 2. Summary of Fixed-Bed Reactor Conditions: $CeO_2$ Sulfidation

| Run | $CeO_2$-01 | $CeO_2$-02 | $CeO_2$-03 | $CeO_2$-04 |
|---|---|---|---|---|
| Date | 03-12-96 | 03-18-96 | 03-26-96 | 03-28-96 |
| Reactor Packing | | | | |
| $CeO_2$, g | 4.00 | 3.35 | 6.04 | 12.61 |
| $Al_2O_3$, g | 4.00 | 3.34 | 3.01 | 3.29 |
| Reaction Conditions | | | | |
| Temp., °C | 300→700 | 650 | 700 | 750 |
| Press., atm | 4.4 | 4.4 | 4.4 | 4.4 |
| Gas Comp. (Nominal) | | | | |
| %$H_2S$ | 1.0 | 1.0 | 1.0 | 1.0 |
| %$H_2$ | 25.0 | 25.0 | 25.0 | 25.0 |
| %$N_2$ | 74.0 | 74.0 | 74.0 | 74.0 |
| Gas Flow, sccm | 600 | 600 | 600 | 298 |
| Space Velocity, $hr^{-1}$ at STP | | 9000 | 7200 | 2000 |

The reaction temperature was increased by 50°C to 700°C in test $CeO_2$-03. This time there was clear evidence that sulfidation occurred, although the extent of reaction was again less than hoped for. Figure 10 compares the $H_2S$ concentration in the product gas as a function of time from run $CeO_2$-03 to the $H_2S$ concentration from an empty reactor (tracer) run at the same temperature, pressure, and feed gas flow rate and composition. In the empty reactor test, $H_2S$ appeared in the product at a mol fraction of 0.0067 in the sample taken about 5.5 minutes after reactive gases were fed to the reactor. From that time the $H_2S$ increased gradually and approached a steady state value of 0.0083 after 60 minutes. The $H_2S$ content during the first 90 minutes of test $CeO_2$-03 increased much more slowly. The difference between the two curves represents $H_2S$ removed by reaction with $CeO_2$.

The empty reactor tracer test was also used to provide information on the delay time at these reaction conditions. Delay time is associated with the elapsed time between opening the valve and feeding reactive gas to the reactor and the time that gas reaches the GC sampling valve. We have defined the delay time as the time required for the product composition to reach 80% of its steady-state value, which is about 5 minutes at the conditions of the empty reactor test.

Although the sulfidation reaction clearly occurred at 700°C (the temperature of run $CeO_2$-03), the rate was much smaller than desired. Consequently, the temperature was increased to 750°C in test $CeO_2$-04. The quantity of $CeO_2$ was doubled and the volumetric flow rate of reactive gas was halved. These changes were all made in the hope of producing the more traditional s-shaped $H_2S$ breakthrough curve. The response from test $CeO_2$-04 is shown in Figure 11, where $H_2S$ mol fraction in the product gas is plotted versus dimensionless time. Dimensionless time for this test is defined as follows

$$t^* = \frac{2\, n_G\, y_{H_2S}\, (t - t_O)}{n_{CeO_2}} \qquad (9)$$

The coefficient 2 is the ratio of the stoichiometric coefficients of $CeO_2$ and $H_2S$, and $t_o$ is the delay time, which is estimated to be 10 minutes based upon the empty reactor tracer test result. $t^*=1$ corresponds to t=4.65 hours.

Large increases in rate of sulfidation and fractional $H_2S$ removal resulted. Greater than 97% of the $H_2S$ was removed for $t^*<0.11$ (t<0.5 hr) and greater than 90% removal was achieved for $t^*<0.42$ (t<2 hrs). The $H_2S$ removal was almost 80% when the run was terminated at $t^*=1.02$ (t=4.74 hrs). The right ordinate of Figure 11 shows the cumulative $H_2S$ removed, as a fraction of the theoretical maximum, versus time. This value was about 0.9 when the run was terminated. These results suggest that a large increase in product gas $H_2S$ concentration should occur if the run had been extended for another 30 to 60 minutes. By that time the conversion of $CeO_2$ to $Ce_2O_2S$ should be complete and the feed and product $H_2S$ concentration should be equal.

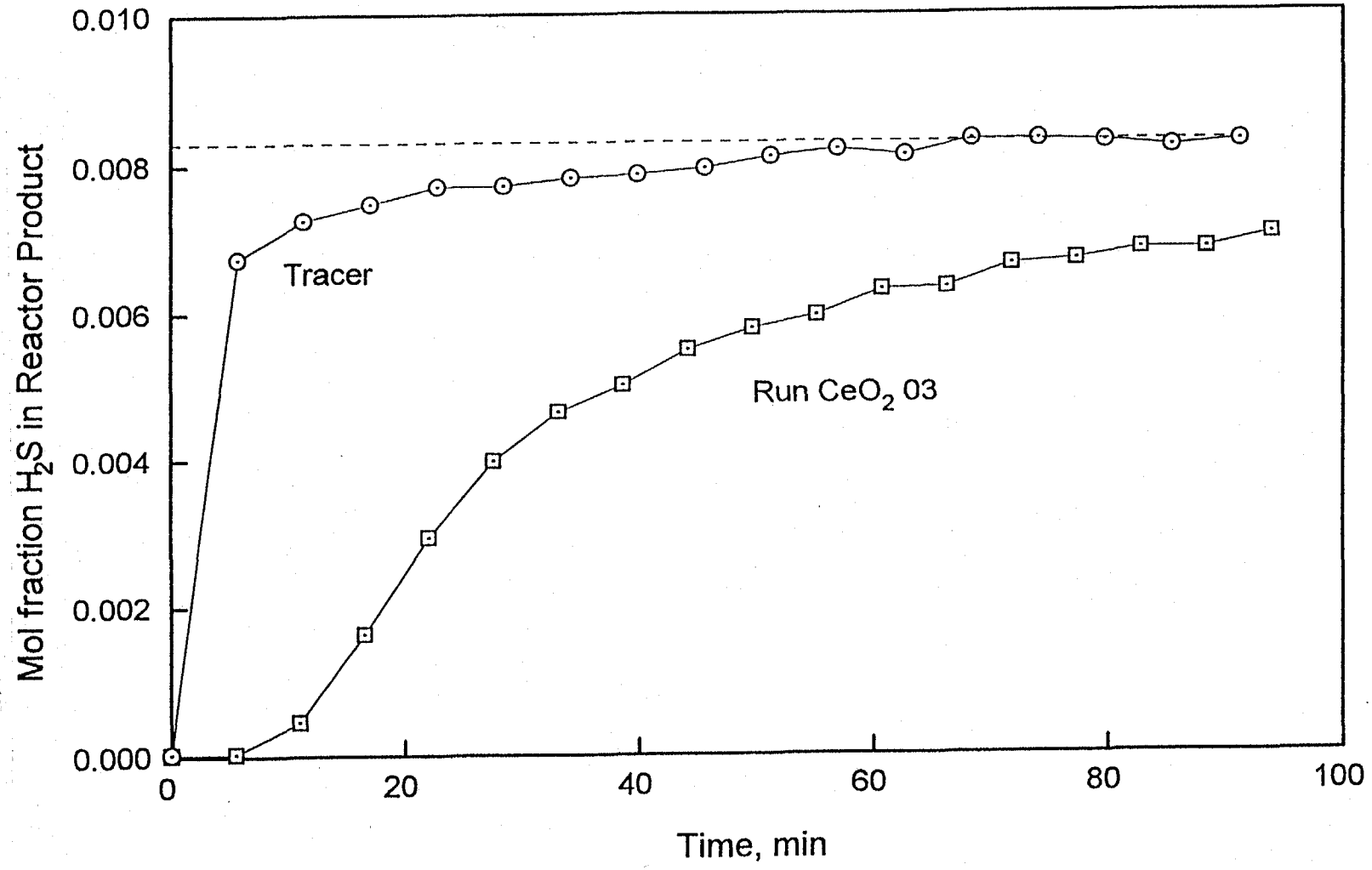


Figure 10. Comparison of Fixed-Bed Reactor Response During Sulfidation of $CeO_2$ (Run $CeO_2$-$O_3$) to the Response Without Sorbent

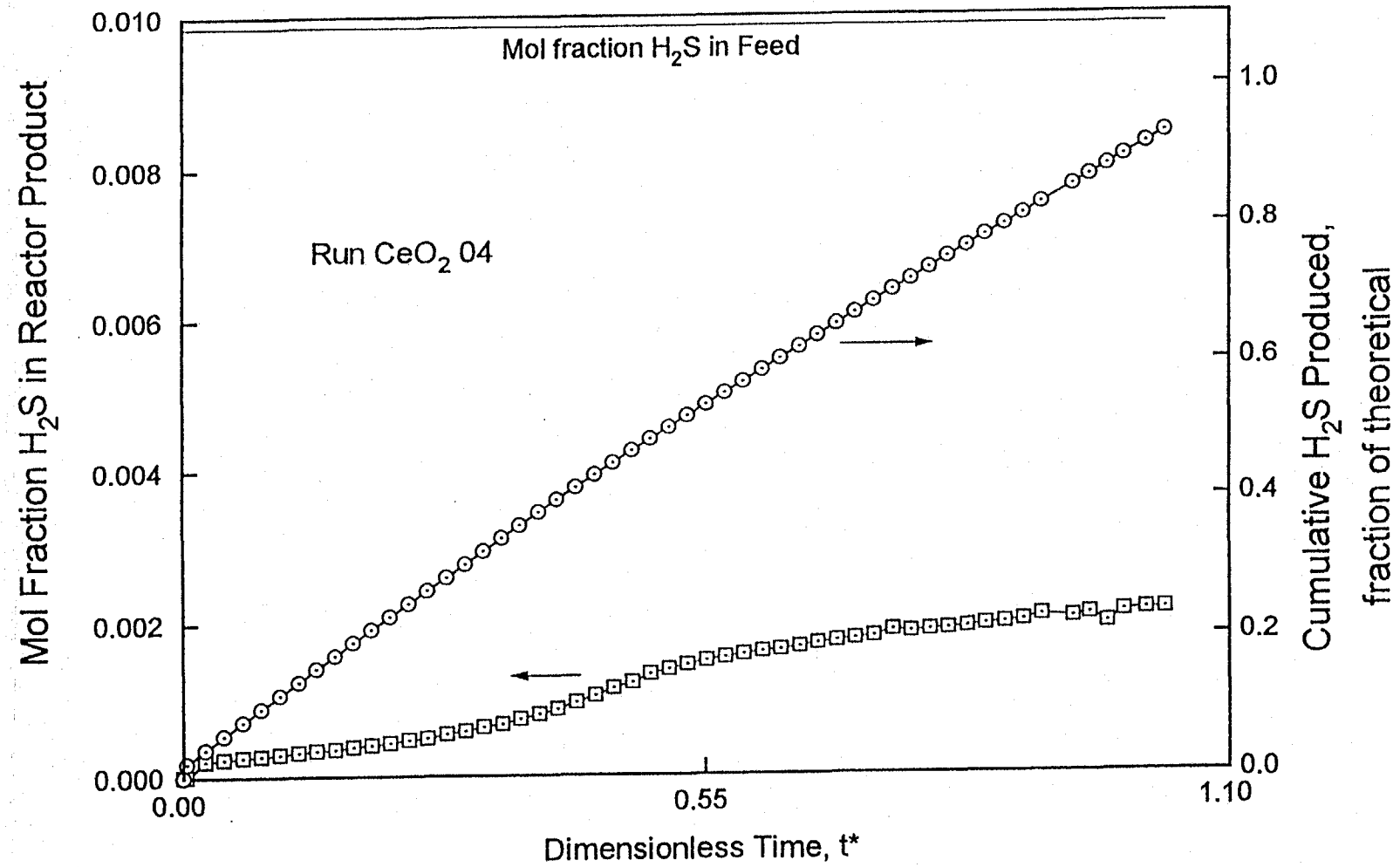


Figure 11. Fixed-Bed Reactor Response: Run $CeO_2$-04

ATMOSPHERIC PRESSURE ELECTROBALANCE

The final atmospheric pressure electrobalance test, which consisted of five regeneration-sulfidation cycles, was completed during the quarter. Reaction conditions are shown below:

Regeneration: $$2FeS + \frac{7}{2}O_2 \rightarrow Fe_2O_3 + 2SO_2 \quad (10)$$

$T = 600°C$
$1\%\ O_2$ in $N_2$

Sulfidation: $$Fe_2O_3 + 2H_2S + H_2 \rightarrow 2FeS + 3H_2O \quad (11)$$

$T=500°C$
$1\%\ H_2S/10\%\ H_2$ in $N_2$

Raw data showing normalized mass, $M/M_o$, versus time is shown in Figures 12 and 13 for the regeneration and sulfidation cycles, respectively. Reference masses for FeS, $Fe_2O_3$, $Fe_3O_4$, FeO, and Fe are shown, as appropriate, for comparison purposes.

The test began with the regeneration of FeS and results are indicated by the cycle 1 curve in Figure 12. The final value of $M/M_o=0.906$ corresponded closely to the theoretical value of 0.908 associated with the conversion of FeS to $Fe_2O_3$. This result was expected as the regeneration conditions were the same as used in many of the earlier single-cycle atmospheric pressure tests. Reaction conditions were then adjusted for the first sulfidation cycle, and results are shown by the cycle 1 curve in Figure 13. Reduction of $Fe_2O_3$ by $H_2$ proceeded simultaneously with sulfidation by $H_2S$. The net result was a loss in mass for the first 15 minutes to a minimum value of $M/M_o=0.772$, followed by an increase to a final value of $M/M_o=0.974$ after 25 minutes. The minimum suggested that the solid at that point consisted of a mixture of Fe, FeO, and FeS. The final value of $M/M_o=0.974$ is consistent with approximately 74% of the iron converted back to FeS.

The second regeneration cycle produced a final value of $M/M_o=0.900$, somewhat smaller than in cycle 1 and also smaller than the theoretical value of 0.908. Mass loss during the early stages of reduction/sulfidation was larger than in cycle 1, and the minimum value of $M/M_o$ was 0.691, again after about 15 minutes. Sulfidation dominated thereafter and the mass increased to a final value of $M/M_o=1.008$, suggesting than essentially all of the iron was converted to FeS. The response during cycle 3 was similar to that of cycle 1 during both the regeneration and reduction/sulfidation phases. The value of $M/M_o$ at the end of reduction was 0.904, the minimum value of $M/M_o=0.763$ during reduction/sulfidation occurred after 15 minutes, and the final of $M/M_o$ was 0.983. Response during the regeneration portions of cycles 4 and 5 was similar to the first three cycles, with final values of $M/M_o=0.900$ and 0.897 in cycles 4 and 5, respectively. However, response during the reduction/sulfidation portions of these two cycles was completely different. There was no initial weight loss, suggesting that $Fe_2O_3$ was not

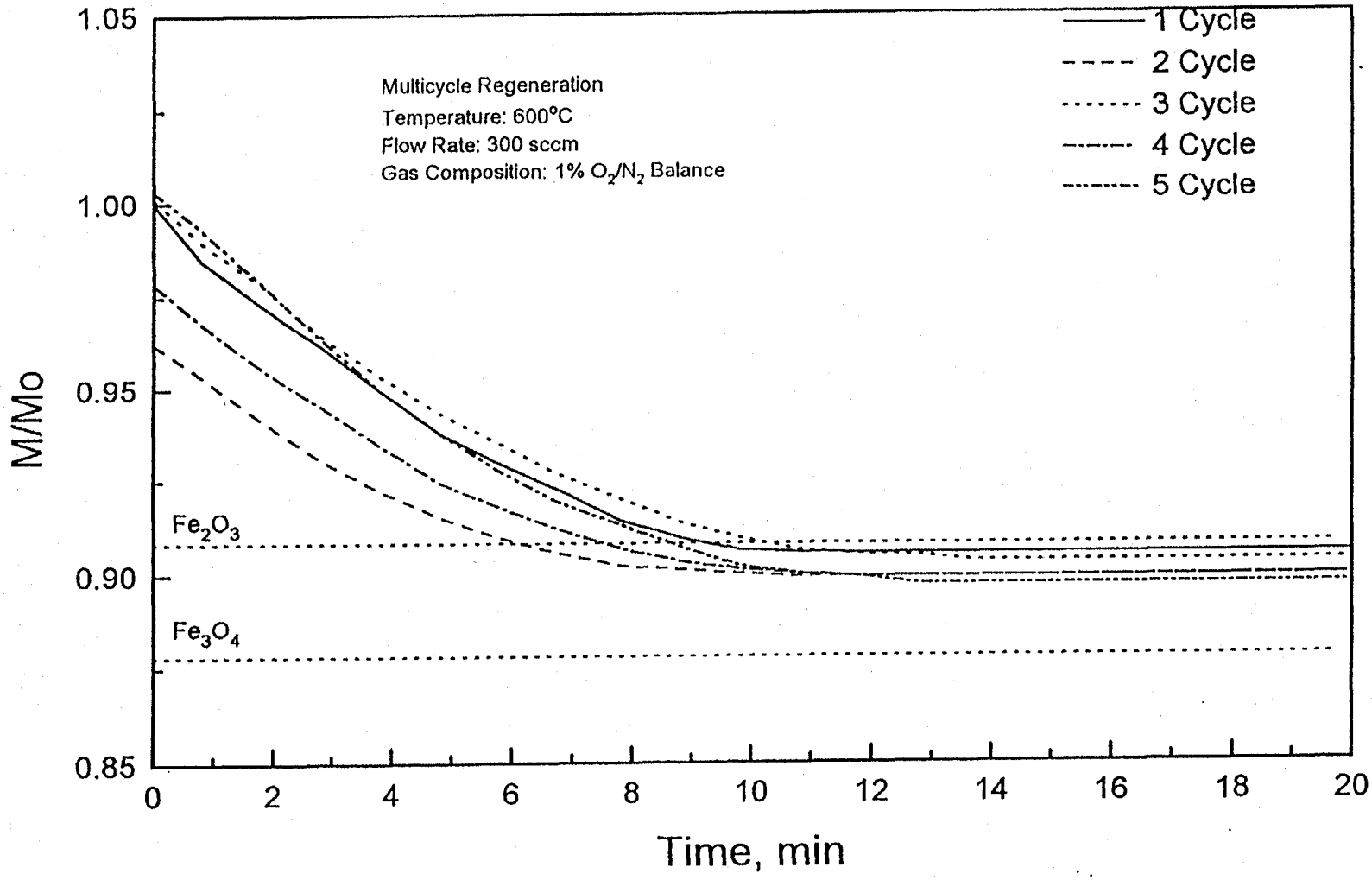


Figure 12. Electrobalance Response Curves for the Regeneration Phase of a Five-Cycle Test

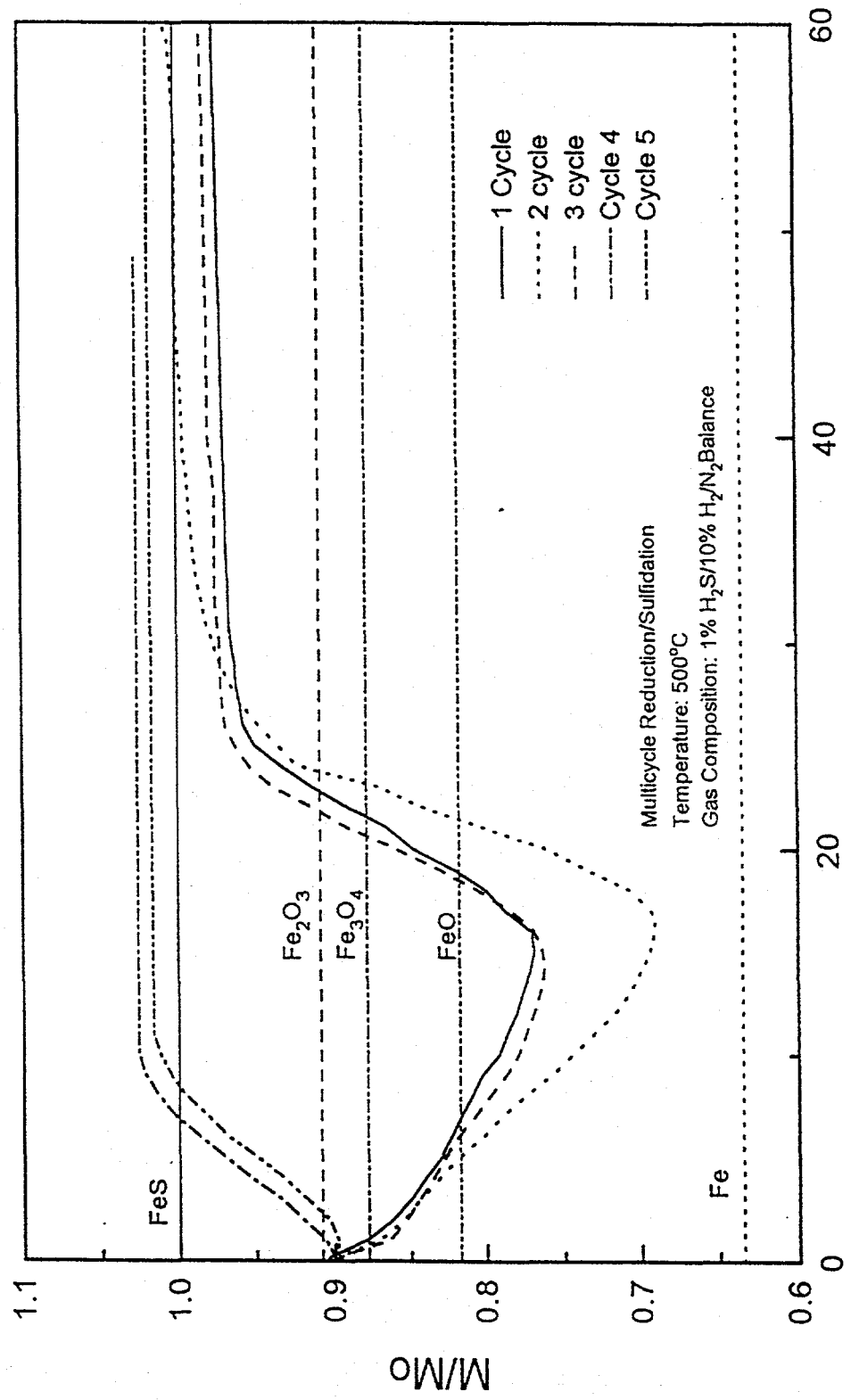


Figure 13. Electrobalance Response Curves of the Reduction--Sulfidation Phase of a Five-Cycle Test

reduced. The final values of $M/M_o$=1.026 and 1.018 in cycles 4 and 5 were both larger than expected.

## HIGH PRESSURE ELECTROBALANCE

Experimental effort using the high pressure electrobalance was also completed during the quarter. The final tests consisted of repeats of a number of $O_2/N_2$ regeneration tests which were carried out early during the test program while procedures and data analysis techniques were being developed. Data scatter in some of these early tests was judged to be excessive and the new tests were meant to reduce the data scatter. Also, a number of experimental regeneration tests in an atmosphere of $O_2/H_2O/N_2$ were carried out. Table 3 summarizes reaction conditions and key results for all $O_2/N_2$ regeneration tests with those completed during the present quarter marked by an asterisk. Similar information for all $O_2/H_2O/N_2$ regeneration tests are presented in Table 4, all of which were completed during the quarter.

An example of the scatter from early $O_2/N_2$ regeneration tests is illustrated in Figure 14 where the initial rate for tests at 1 atm is plotted as a function of $O_2$ mol fraction and temperature. More detailed information on these early tests is presented in the columns of Table 5 labeled "original test results," where the slopes of the initial rate versus $O_2$ mol fraction curves plus/minus the standard deviation of the slope is presented for each temperature and pressure combination. The data shown in Figure 14 corresponds to the Table 5 entries under "original test results" at 1 atm. Figure 14, in addition to indicating greater data scatter than desired, shows that the initial reaction rate decreased with increasing temperature between 600 and 700°C. While the initial rate was not expected to be a strong function of temperature, there is no way to justify a decrease in rate with increasing temperature.

The results from Figure 14 which were most suspect were from the two tests at 600°C and 3% $O_2$ (tests F37 and F38), both of which were conducted early in the experimental program and both initial rates were significantly larger than expected. As a consequence, a repeat test, F88, was conducted at 600°C, 3% $O_2$, and 1 atm. This test produced a smaller initial rate as shown in Table 3. Other reaction conditions at which repeat tests were conducted are noted by the asterisk adjacent to the temperature in Table 5. Slopes and standard deviations of the slopes for the "original plus new test results" are shown by the central columns of Table 5. In some cases, for example at 600°C and 1 atm, addition of the new test results produced a significant decrease in the slope and standard deviation. In other cases, for example at 800°C and 15 atm, addition of the new results produced little or no change in slope and standard deviation. Finally, when the suspect early results were deleted and replaced by the new results, regression of the data produced the slopes and standard deviations shown in Table 5 under the heading"results after deleting suspect old data." In most cases, this produced a further reduction in both the slopes and standard deviations. As a result, the initial rate increased with increasing temperature at all pressures.

Table 3. Operating Conditions and Key Results for High Pressure Electrobalance Tests Involving the Regeneration of FeS in $O_2/N_2$

| | Date | Run | T | Qt | O2 | P | Mo | M1 | M2 | M1/Mo | M2/Mo | Rate |
|---|---|---|---|---|---|---|---|---|---|---|---|---|
| | | | (C) | (sccm) | (%) | (atm) | (mg) | (mg) | (mg) | | | (min^-1) |
| | 7/31/95 | F 37 | 600 | 800 | 3.0 | 1 | 2.545 | 2.311 | | 0.908 | | 0.0400 |
| | 7/31/95 | F 38 | 600 | 1000 | 3.0 | 1 | 2.380 | 2.161 | | 0.908 | | 0.0483 |
| | 8/1/95 | F 39 | 800 | 1000 | 3.0 | 15 | 2.898 | 2.631 | | 0.908 | | 0.0350 |
| | 8/1/95 | F 40 | 800 | 800 | 3.0 | 15 | 3.920 | 3.559 | | 0.908 | | 0.0350 |
| | 8/15/95 | F 42 | 700 | 800 | 3.0 | 15 | 2.540 | 2.304 | | 0.907 | | 0.0300 |
| | 8/16/95 | F 43 | 650 | 800 | 3.0 | 15 | 3.060 | 2.739 | | 0.895 | | 0.0125 |
| | 8/17/95 | F 44 | 625 | 800 | 3.0 | 15 | 3.360 | 3.064 | | 0.912 | | 0.0125 |
| | 8/17/95 | F 45 | 600 | 800 | 3.0 | 15 | 3.048 | 2.926 | | 0.960 | | 0.0214 |
| | 8/22/95 | F 47 | 600 | 800 | 1.0 | 1 | 2.910 | 2.619 | | 0.900 | | 0.0100 |
| | 8/22/95 | F 48 | 700 | 800 | 0.5 | 1 | 3.470 | 3.151 | | 0.908 | | 0.0059 |
| | 8/22/95 | F 49 | 700 | 800 | 1.0 | 1 | 3.060 | 2.754 | | 0.900 | | 0.0114 |
| | 8/23/95 | F 50 | 700 | 800 | 3.0 | 1 | 3.920 | 3.559 | | 0.908 | | 0.0358 |
| | 8/24/95 | F 51 | 700 | 800 | 0.5 | 1 | 2.934 | 2.655 | | 0.905 | | 0.0060 |
| | 8/24/95 | F 52 | 600 | 800 | 0.5 | 1 | 2.900 | 2.633 | | 0.908 | | 0.0056 |
| | 8/25/95 | F 53 | 800 | 800 | 1.0 | 1 | 2.734 | 2.485 | | 0.909 | | 0.0150 |
| | 8/28/95 | F 54 | 600 | 800 | 1.0 | 5 | 2.572 | 2.335 | | 0.908 | | 0.0180 |
| | 8/28/95 | F 55 | 700 | 800 | 0.5 | 5 | 2.275 | 2.052 | | 0.902 | | 0.0067 |
| | 8/29/95 | F 56 | 700 | 800 | 1.0 | 5 | 2.284 | 2.062 | | 0.903 | | 0.0175 |
| | 8/29/95 | F 57 | 700 | 800 | 3.0 | 5 | 2.117 | 1.916 | | 0.905 | | 0.0400 |
| | 8/30/95 | F 58 | 700 | 800 | 3.0 | 5 | 3.004 | 2.704 | | 0.900 | | 0.0400 |
| | 9/1/95 | F 59 | 800 | 800 | 1.0 | 5 | 4.310 | 3.879 | | 0.900 | | 0.0164 |
| | 9/5/95 | F 60 | 700 | 800 | 0.5 | 15 | 3.006 | 2.705 | | 0.900 | | 0.0067 |
| | 9/6/95 | F 61 | 700 | 800 | 1.0 | 15 | 2.436 | 2.192 | | 0.900 | | 0.0150 |
| | 9/6/95 | F 62 | 800 | 800 | 0.5 | 1 | 3.520 | 3.168 | | 0.900 | | 0.0082 |
| | 9/7/95 | F 63 | 800 | 800 | 3.0 | 1 | 3.034 | 2.731 | | 0.900 | | 0.0429 |
| | 9/7/95 | F 64 | 600 | 800 | 0.5 | 5 | 4.680 | 4.212 | | 0.900 | | 0.0092 |
| | 9/8/95 | F 65 | 600 | 800 | 3.0 | 5 | 2.916 | 2.654 | | 0.910 | | 0.0450 |
| | 9/8/95 | F 66 | 800 | 800 | 0.5 | 5 | 4.510 | 4.104 | | 0.910 | | 0.0078 |
| | 9/11/95 | F 67 | 800 | 800 | 3.0 | 5 | 2.791 | 2.512 | | 0.900 | | 0.0467 |
| | 9/11/95 | F 68 | 600 | 800 | 0.5 | 15 | 2.469 | 2.247 | | 0.910 | | 0.0045 |
| | 9/12/95 | F 69 | 600 | 800 | 1.0 | 15 | 3.195 | 2.994 | | 0.937 | | 0.0060 |
| | 9/13/95 | F 70 | 800 | 800 | 0.5 | 15 | 3.450 | 3.105 | | 0.900 | | 0.0054 |
| | 9/22/95 | F 75 | 600 | 800 | 1.0 | 1 | 4.600 | 4.140 | | 0.900 | | 0.0100 |
| | 10/9/95 | F 81 | 700 | 800 | 0.5 | 1 | 3.159 | 2.859 | | 0.905 | | 0.0072 |
| | 10/9/95 | F 82 | 600 | 800 | 3.0 | 5 | 4.340 | 3.949 | | 0.910 | | 0.0360 |
| | 10/10/95 | F 83 | 800 | 800 | 1.0 | 15 | 2.988 | 2.704 | | 0.905 | | 0.0150 |
| | 10/11/95 | F 84 | 600 | 800 | 3.0 | 5 | 2.796 | 2.533 | | 0.906 | | 0.0400 |
| | 10/12/95 | F 85 | 800 | 800 | 1.0 | 15 | 3.157 | 2.873 | | 0.910 | | 0.0188 |
| | 10/13/95 | F 86 | 700 | 800 | 0.5 | 1 | 2.527 | 2.274 | | 0.900 | | 0.0064 |
| | 10/16/95 | F 87 | 700 | 800 | 0.5 | 1 | 2.775 | 2.498 | | 0.900 | | 0.0068 |
| * | 1/4/96 | F 88 | 800 | 600 | 3.0 | 1 | 2.736 | 2.462 | | 0.900 | | 0.0300 |
| * | 1/4/96 | F 89 | 800 | 600 | 1.0 | 5 | 3.640 | 3.276 | | 0.900 | | 0.0120 |
| * | 1/5/96 | F 90 | 800 | 700 | 1.0 | 5 | 3.340 | 3.006 | | 0.900 | | 0.0140 |
| * | 1/16/96 | F 91 | 800 | 600 | 0.5 | 5 | 2.987 | 2.688 | | 0.900 | | 0.0057 |
| * | 1/17/96 | F 92 | 800 | 700 | 0.5 | 15 | 2.216 | 1.997 | | 0.901 | | 0.0057 |
| * | 1/18/96 | F 93 | 800 | 700 | 1.0 | 15 | 2.765 | 2.489 | | 0.900 | | 0.0110 |
| * | 1/19/96 | F 94 | 800 | 800 | 0.5 | 15 | 3.012 | 2.726 | | 0.905 | | 0.0070 |
| * | 1/20/96 | F 95 | 800 | 700 | 3.0 | 5 | 3.260 | 2.934 | | 0.900 | | 0.0420 |
| * | 2/15/96 | F 96 | 600 | 800 | 3.0 | 1 | 2.374 | 2.148 | | 0.905 | | 0.0290 |
| * | 2/16/96 | F 97 | 700 | 800 | 3.0 | 1 | 2.360 | 2.126 | | 0.901 | | 0.0380 |
| * | 2/16/96 | F 98 | 800 | 800 | 3.0 | 1 | 3.720 | 3.348 | | 0.900 | | 0.0420 |

Table 4. Operating Conditions and Key Results for High Pressure Electrobalance Tests Involving the Regeneration of FeS in $O_2/H_2O/N_2$

| | Date | Run | T | Qt | H2O | O2 | P | Mo | M1 | M2 | M1/Mo | M2/Mo | Rate |
|---|---|---|---|---|---|---|---|---|---|---|---|---|---|
| | | | (C) | (sccm) | (%) | (%) | (atm) | (mg) | (mg) | (mg) | | | (min^-1) |
| * | 1/22/96 | C 01 | 700 | 800 | 30 | 0.05 | 1 | 2.152 | 1.937 | | 0.900 | | 0.0062 |
| * | 1/23/96 | C 02 | 700 | 800 | 30 | 0.30 | 1 | 2.954 | 2.662 | | 0.901 | | 0.0100 |
| * | 1/24/96 | C 03 | 700 | 800 | 30 | 0.50 | 1 | 2.714 | 2.443 | | 0.900 | | 0.0120 |
| * | 1/25/96 | C 04 | 600 | 800 | 30 | 0.30 | 1 | 3.012 | 2.711 | | 0.900 | | 0.0060 |
| * | 1/26/96 | C 05 | 800 | 800 | 30 | 0.30 | 1 | 2.997 | 2.697 | | 0.900 | | 0.0150 |
| * | 2/1/96 | C 06 | 700 | 800 | 30 | 0.05 | 5 | 2.314 | 2.087 | | 0.902 | | 0.0110 |
| * | 2/2/96 | C 07 | 700 | 800 | 30 | 0.30 | 5 | 3.260 | 2.934 | | 0.900 | | 0.0140 |
| * | 2/5/96 | C 08 | 700 | 800 | 30 | 0.50 | 5 | 3.780 | 3.402 | | 0.900 | | 0.0170 |
| * | 2/6/96 | C 09 | 600 | 800 | 30 | 0.30 | 5 | 2.970 | 2.673 | | 0.900 | | 0.0090 |
| * | 2/7/96 | C 10 | 800 | 800 | 30 | 0.30 | 5 | 3.800 | 3.420 | | 0.900 | | 0.0180 |
| * | 2/8/96 | C 11 | 700 | 800 | 30 | 0.05 | 15 | 2.135 | 1.922 | | 0.900 | | 0.0040 |
| * | 2/9/96 | C 12 | 700 | 800 | 30 | 0.30 | 15 | 3.151 | 2.852 | | 0.905 | | 0.0070 |
| * | 2/12/96 | C 13 | 700 | 800 | 30 | 0.50 | 15 | 2.128 | 1.936 | | 0.910 | | 0.0100 |
| * | 2/13/96 | C 14 | 600 | 800 | 30 | 0.30 | 15 | 3.214 | 2.893 | | 0.900 | | 0.0040 |
| * | 2/14/96 | C 15 | 800 | 800 | 30 | 0.30 | 15 | 3.830 | 3.447 | | 0.900 | | 0.0100 |

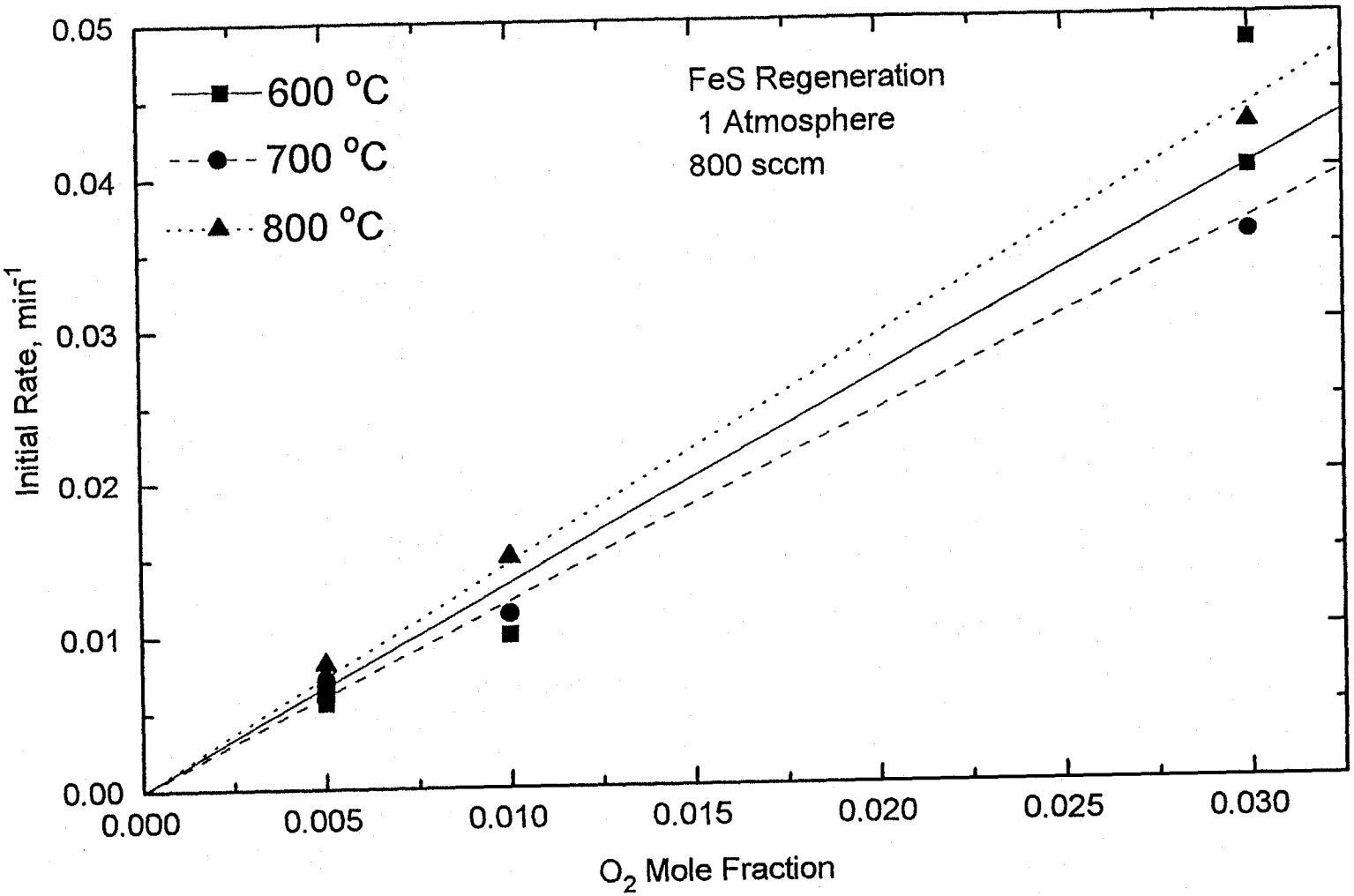


Figure 14. Results of Early Tests Showing the Effect of $O_2$ Mol Fraction and Temperature on the Initial Rate: P=1 atm

Table 5. Comparison of $O_2/N_2$ Regeneration Rates as a Function of Temperature and Pressure

| | Original Test Results | | Original Plus New Test Results | | Results After Deleting Some of Old Data | |
|---|---|---|---|---|---|---|
| T, °C | Slope | Std. Dev. | Slope | Std. Dev. | Slope | Std. Dev. |
| P = 1 atm | | | | | | |
| 600* | 1.34 | 0.07 | 1.25 | 0.06 | 1.01 | 0.01 |
| 700 | 1.22 | 0.01 | 1.22 | 0.01 | 1.22 | 0.01 |
| 800 | 1.47 | 0.05 | 1.47 | 0.05 | 1.47 | 0.05 |
| P = 5 atm | | | | | | |
| 600* | 1.41 | 0.05 | 1.38 | 0.03 | 1.25 | 0.03 |
| 700* | 1.39 | 0.05 | 1.39 | 0.02 | 1.40 | 0.00 |
| 800 | 1.58 | 0.03 | 1.58 | 0.03 | 1.58 | 0.03 |
| P = 15 atm | | | | | | |
| 600 | -- | -- | -- | -- | -- | -- |
| 700* | 1.15 | 0.18 | 1.14 | 0.06 | 1.04 | 0.04 |
| 800* | 1.38 | 0.07 | 1.38 | 0.06 | 1.23 | 0.04 |

The effect of temperature on the initial rate, using data from the columns headed "results after deleting suspect old data," was then examined using the Arrhenius equation. Results are shown in Figure 15, with each line corresponding to a different operating pressure. The slopes and intercepts of the lines were used to determine the activation energy and frequency factor. The final equations used for predicting the initial regeneration rate of FeS in $O_2/N_2$ are:

$$P = 1 \text{ atm} \qquad r_o = 7.43\, e^{-3470/RT}\, y_{O_2} \tag{12}$$

$$P = 5 \text{ atm} \qquad r_O = 3.66\, e^{-1820/RT}\, y_{O_2} \tag{13}$$

$$P = 15 \text{ atm} \qquad r_o = 4.65^{-1442/RT}\, y_{O_2} \tag{14}$$

A similar approach to data analysis for the initial reaction rate in $H_2O/N_2$ was carried out. However, none of these tests was repeated. Figure 16 shows the Arrhenius plot for $H_2O/N_2$ regeneration at the three pressures. The final rate equations for $H_2$) regeneration are:

$$P = 1 \text{ atm} \qquad r_{H_2O} = 5.0\, e^{-10,640/RT}\, y_{H_2O} \tag{15}$$

$$P = 5 \text{ atm} \qquad r_{H_2O} = 2.58\, e^{-8540/RT}\, y_{H_2O} \tag{16}$$

$$P = 15 \text{ atm} \qquad r_{H_2O} = 1.52\, e^{-9700/RT}\, y_{H_2O} \tag{17}$$

The activation energies for steam regeneration are, as expected, larger than the activation energies for $O_2$ regeneration. The initial rates for steam regeneration, however, are much smaller. For example, at 700°C and 5 atm, the initial rate in $O_2$ is 136 times larger than the initial rate in $H_2O$. At 800°C and 5 atm, the ratio of the initial rates is reduced to 89 because of the larger activation energy associated with $H_2O$ regeneration.

Comparable rate equations at 1 atm using results from the atmospheric pressure electrobalance tests were reported in the previous quarterly report. The equations for $H_2O$ regeneration in the 1 atm tests from the two electrobalances agreed quite well with each other. The difference was less than 5% over the 600°C - 800°C temperature range. However, the initial rates for $O_2$ regeneration were about 30% larger from the atmospheric pressure electrobalance.

The limited series of tests involving regeneration in $O_2/H_2O/N_2$ were, as shown in Table 4, all conducted using 30% $H_2O$ in the feed gas. The oxygen content was varied between 0.0005 and 0.005 mol fraction in insure that the initial rate with steam would contribute a significant portion of the total initial rate. The temperature and pressure ranges were 600°C to 800°C and 1 atm to 15 atm, respectively.

The two reactions were found to be found to be independent in that the measured total rate was equal to the sum of the individual rates. This is illustrated in Figure 17 where the experimental initial rate at 700°C is plotted versus mol fraction $O_2$ for each operating pressure. Experimental results are indicated by the individual points, while the continuous lines represent expected rates based on summing the predicted rates of $O_2$ regeneration and $H_2O$ regeneration.

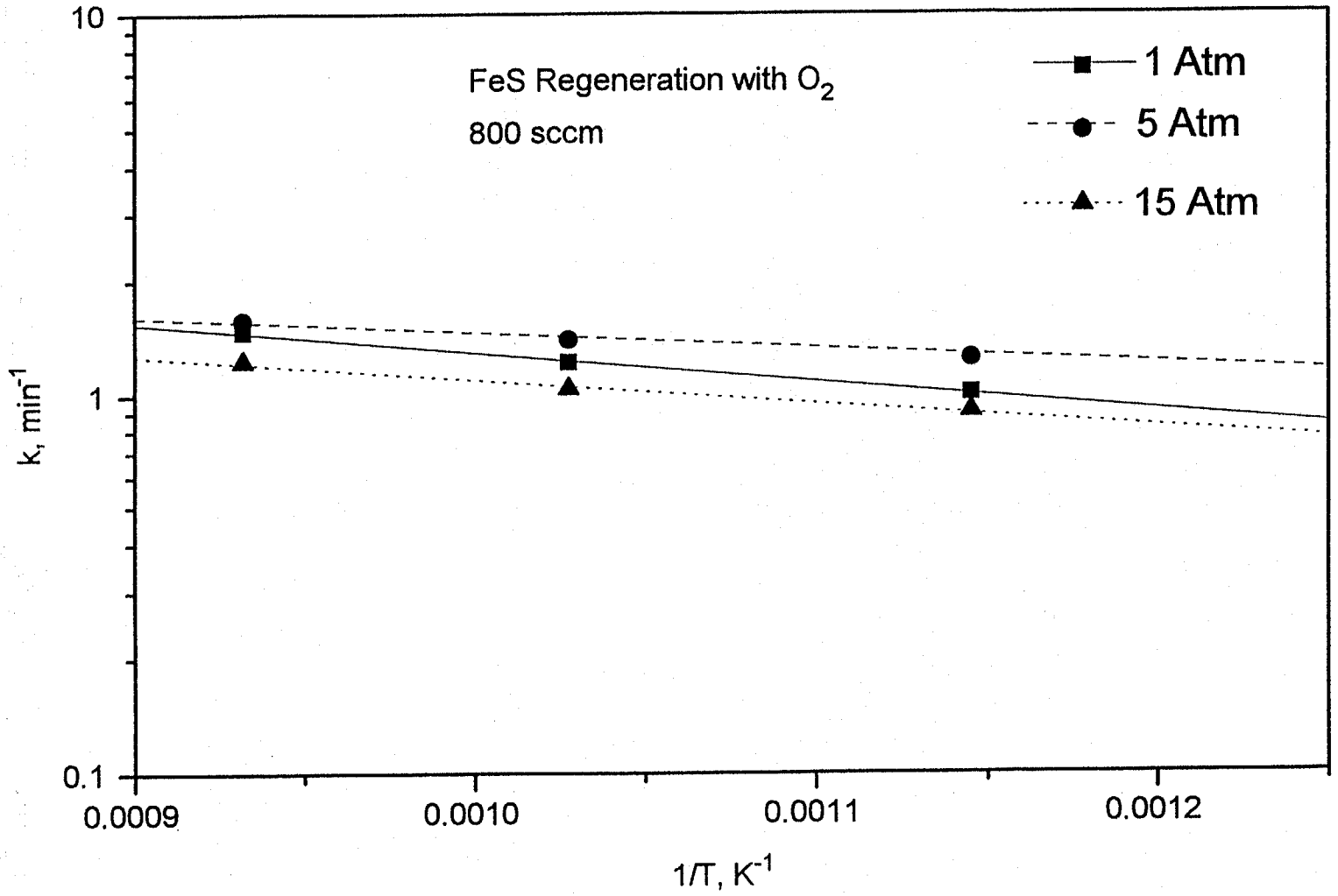


Figure 15. Arrhenius Analysis of the Effect of Temperature on the Initial Rate of Regeneration of FeS in $O_2/N_2$

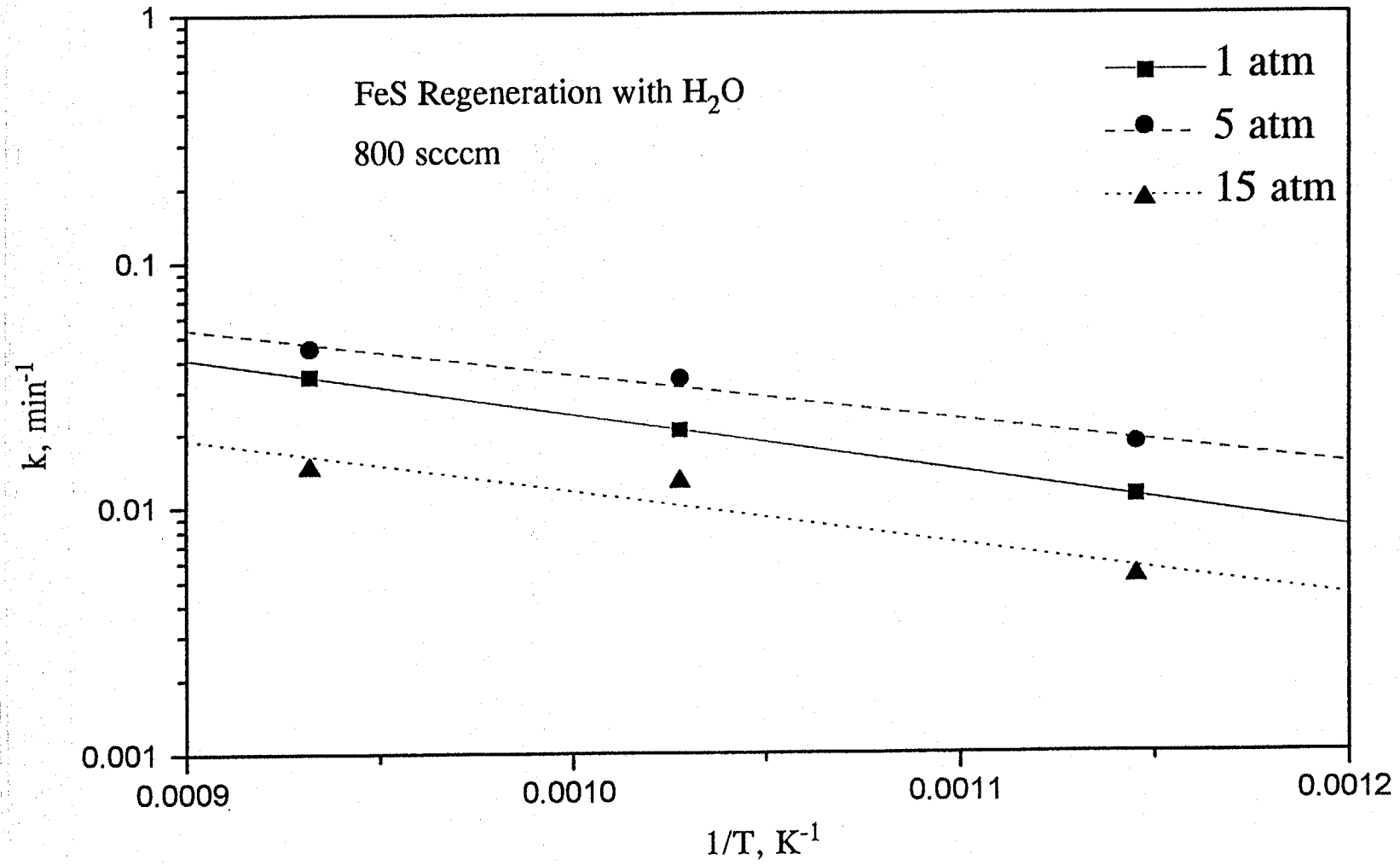


Figure 16. Arrhenius Analysis of the Effect of Temperature on the Initial Rate of Regeneration of FeS in $H_2O/N_2$

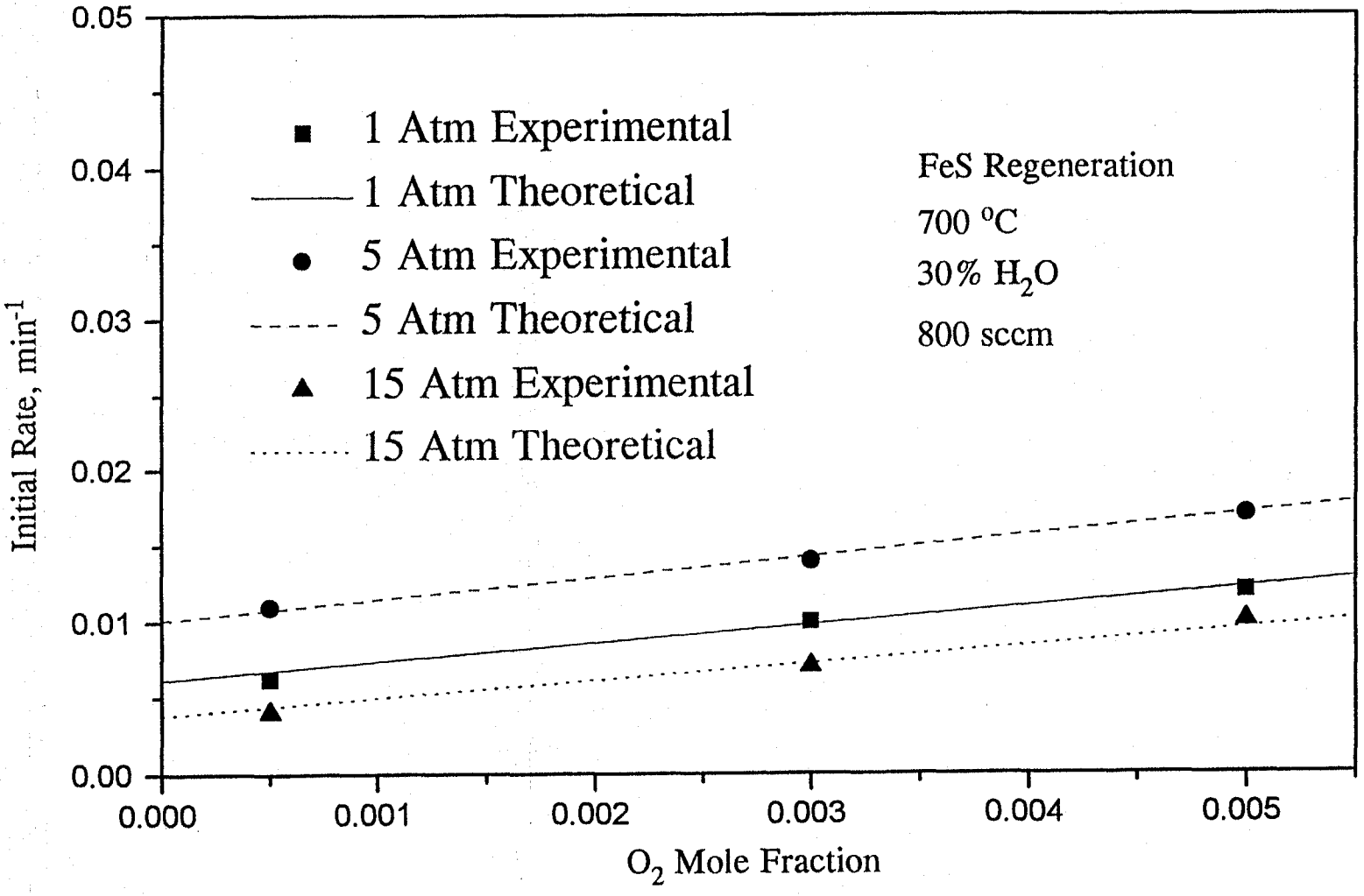


Figure 17. Comparison of Experimental and Predicted Initial Rates for the Regeneration of FeS in $O_2/H_2O/N_2$